

Shoreline Impacts Study for Sabine Neches Project

**Mark Gravens
David B. King**

January 2003

Coastal and Hydraulics Laboratory
US Army Corps of Engineers
Engineer Research and Development Center, Vicksburg

STUDY OF SHORELINE IMPACTS DUE TO PROPOSED DEEPENING OF THE SABINE PASS ENTRANCE CHANNEL, SABINE, TX

I. INTRODUCTION

The navigation channel leading to the port of Sabine, TX, currently extends some 18.1 miles (29.2 km) into the Gulf of Mexico and has an authorized depth of 40 ft (12.2 m). The US Army Engineer District, Galveston, (SWG) is studying three proposals to deepen the channel: to 45 ft (13.7 m), to 48 ft (14.6 m), or to 50 ft (15.2 m). These three alternatives would lengthen the current channel to 30.5 miles (49.1 km), 31.3 miles, (50.4 km) or 32 miles (51.5 km), respectively. This study examines potential project impacts on adjacent shorelines due to changes in waves and sediment transport caused by the proposed channel modifications. Specifically, the study focuses on the changes that would occur in wave heights, wave angles, sediment transport rates, and shoreline positions if a deeper channel were constructed.

The spectral near shore wave transformation model, STWAVE, was applied to examine wave conditions within a bathymetry grid extending 20 miles (32 km) along shore (centered at Sabine Pass) and extending 45.5 miles (73.2 km) offshore. Input waves for this model were developed from a 10-year hindcast of Gulf of Mexico wave conditions. The wave conditions near the shoreline, which were an output of the STWAVE model, were used as input to the shoreline change model, GENESIS.

This investigation examined the 45 and 50 ft channel alternatives in detail. The 48 ft channel was not specifically addressed. However, in all cases, the project-induced changes in going from a 40 to a 45 ft channel were less than the corresponding changes in going from a 40 to a 50 ft channel. It is reasonable, therefore, to assume that the changes in going to a 48 ft channel would be intermediate to the changes quantified for the 45 and 50 ft design alternatives.

IIA. DATA SOURCES - BATHYMETRY

Bathymetry data were obtained from NOS hydrographic surveys that were available in electronic format from the Geophysical Data System (GEODAS, ver. 4.0) developed by the National Geophysical Data Center. GEODAS is an interactive database management system for use in the assimilation, storage, and retrieval of geophysical data. There was good bathymetric coverage of the area offshore of Sabine Pass collected in the 1960's and 1970's, so these surveys were selected as the primary bathymetry data sets, with earlier 1937 surveys used to fill gaps. These surveys are listed in Table 1. Vertical survey datums were adjusted from MLW to NAVD88 using the correction from the Galveston Pleasure Pier (NOAA Tide Station 8771510, Latitude 29° 17.1' N, Longitude 94° 47.3' W) by adding 0.19 feet of depth. Horizontal survey datums were converted to NAD83, Texas State Plane Coordinate System, South Central Zone 4204.

NGDC #	Survey	Soundings	Date	Datum	Datum Ref	Location
3071075	H08712	14557	1962	MLW	NAD27	SABINE BANK
3071077	H08737	5599	1963	MLW	NAD27	HEALD BANK
3071078	H08738	12359	1963	MLW	NAD27	SOUTH OF SABINE BANK
3071079	H08739	11672	1963	MLW	NAD27	SABINE BANK
3071080	H08767	4214	1962	MLW	NAD27	SABINE BANK
3071082	H08795	16438	1964	MLW	NAD27	SABINE BANK
3071083	H08796	23068	1964	MLW	NAD27	SABINE BANK
3091061	H09765	23172	1978	MLW	NAD27	OFFSHORE GILCHRIST, TX
3091062	H09769	10496	1978	MLW	NAD27	VICINITY OF HIGH ISLAND
3091063	H09774	20025	1978	MLW	NAD27	OFFSHORE GALVESTON
3091064	H09775	23060	1978	MLW	NAD27	WEST OF HEALD BANK
3091066	H09784	23285	1978	MLW	NAD27	SOUTHEAST OF GALVESTON
3091067	H09785	12371	1978	MLW	NAD27	CALCASIEU PASS TO SABINE PASS
3091072	H09851	22	1979	MLW	NAD27	OFFSHORE GALVESTON
3071042	H06251	11561	1937	MLW	NAD27	BOLIVAR PENIN TO HEALD BANK
3071045	H06294	4094	1937	MLW	NAD27	SOUTHEAST OF SABINE BANK

Table 1 - Hydrographic data sources.

Recent channel surveys were supplied by SWG. These were converted from MLT datum to NAVD88 by adding 0.80 feet of depth. The surveys showed typical channel depths to be about 46 ft. along the length of the channel. This represents the present authorized depth of 40 ft., plus 2 ft. of advanced maintenance, 2 ft. allowance for wave action, and 2 ft. of allowable over-depth. For the proposed 50 ft channel, the bathymetry was modified to include a 56 ft deep, 800 ft wide channel along the first 18.1 miles (the present channel length) and a 56 ft deep, 700 ft wide channel out to 32.0 miles. For the proposed 45 ft channel, the bathymetry was modified to include a 51 ft deep, 800 ft wide channel for the first 18.1 miles, and a 51 ft deep 700 ft wide channel out to 30.5 miles.

Using the bathymetry, a study grid was laid out that extended 105,600 ft (20 miles, 32 km) along shore, centered at Sabine Pass, and extended 240,000 ft (45.5 miles, 73.2 km) offshore to approximately the -66 ft (-20 m) bathymetry contour. To properly resolve the 800 ft (244 m) wide channel, the grid spacing in both the along-shore and offshore directions was set at 160 ft (48.8 m). Thus, the grid was 661 cells wide in the along-shore direction by 1501 cells long in the offshore direction. The bathymetry and the grid are shown in Figure 1.

Figure 1A shows the shoreline (in white) from near High Island in the west (left), past Sabine Pass in the middle, to near Calcasieu Pass in the east (right). Bathymetry contours are shown in green. From top to bottom, the first dark green band is the 15 ft depth contour. The first light green band is the 30 ft depth contour. The next light green enclosed area is Sabine Bank, where the bottom rises to less than a 30 ft depth. Seaward of this bank are the 45, 60, and 75 ft depth contours (dark, light, and dark green). The existing channel is shown in red and the proposed extension in purple (50 ft alternative). The yellow box is the boundary of the computational wave grid. The blue circle is the location of the WIS wave data station.

Figure 1B shows the bathymetry within the computational wave grid (the yellow box in Figure 1A). The shore is shown in gray, with the shoreline and the proposed channel in brown. Shallow bathymetry is shown in yellow, and deep in blue. The depth scale to the right is in

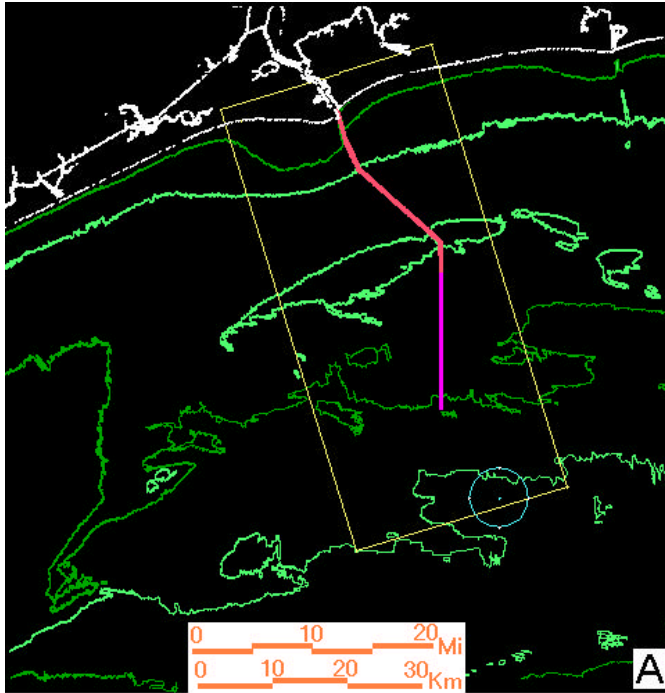


Figure 1A - Gulf of Mexico Bathymetry Near Sabine Pass.

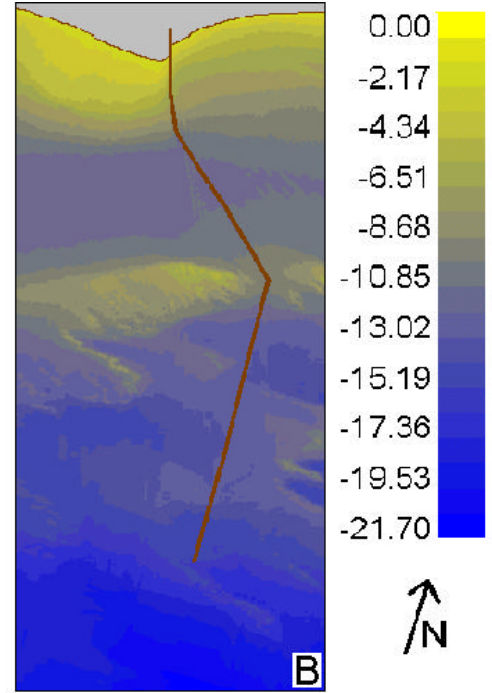


Figure 1B - Computational Wave Grid Bathymetry.

meters. Note the prominence of Sabine Bank in the middle of the figure. For length scales, the dimensions of the Figure 1B box are 105,600 ft by 240000 ft. The straight offshore direction is 164° clockwise from North.

IIB. WAVE DATA

The ambient wave climate at the seaward edge of the grid was obtained from a 10-year hindcast (1990-1999) of wave conditions at WIS station GOM 093, whose location is shown in Figure 1A. The wave climatology offshore of Sabine Pass was characterized by representative wave events in 30 unique wave direction / period bands. Each representative wave event was developed as the average wave angle and wave period of all waves in that angle band and period band. The frequency of occurrence in each of 30 bins is shown in Figure 2 and Table 2. The period boundaries for the bins are 3, 4, 5, 7, 9, 11, and 15 seconds. The angle boundaries are 90° , 25° , 5° , -5° , -25° , and -90° . Each of these 30 representative wave cases was transformed across the computational grid shown in Figure 1B using STWAVE.

In Figure 2, the numbers in the center of each bin or case are the frequency of occurrence in percent. Bright yellow cases occur most frequently, bright blue, least frequently. In this text, cases are referred to by their case number, the gray background number in the upper left corner of each case. The wave angle convention is such that positive angles are those approaching the coast from the east; negative angles approach the coast from the southwest. The zero angle is the shore normal direction.

Percent Occurrence

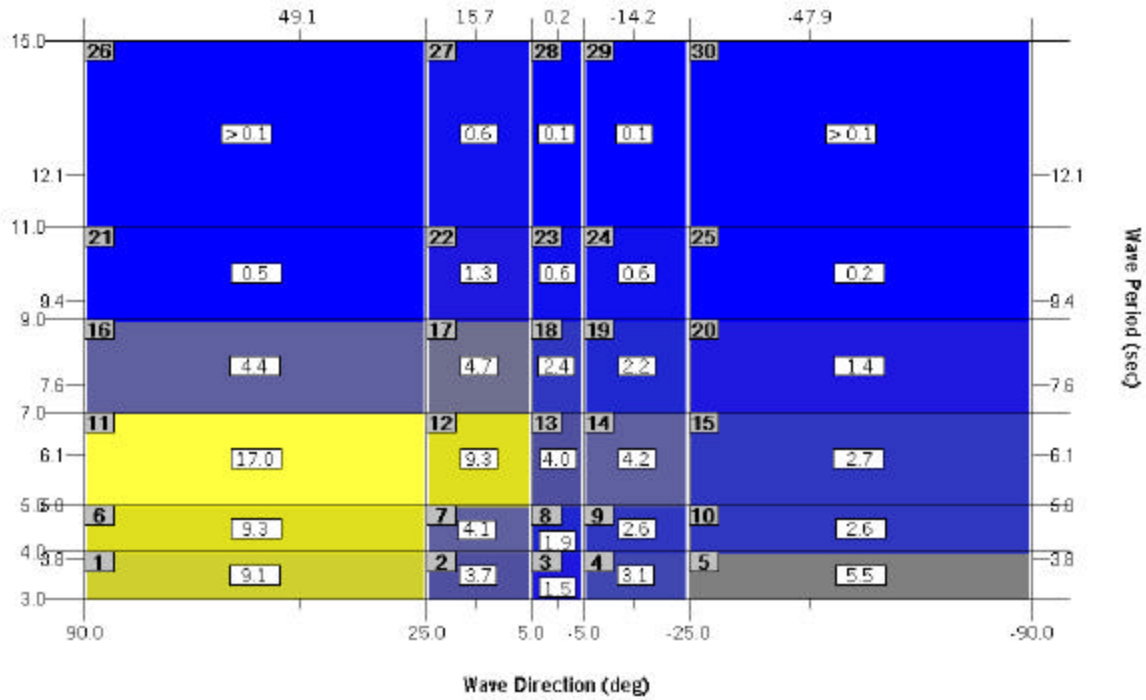


Figure 2 - Wave Direction and Period Bins or Cases.

Case #	Wave period	Wave angle	% Occurrence	Cumulative % Occurrence
11	5.95	40°	17.0	17.0
6	4.90	40°	9.3	26.3
12	5.95	15°	9.3	35.7
1	3.75	40°	9.1	44.8
5	3.75	-40°	5.5	50.3
17	7.58	15°	4.7	55.0
16	7.58	40°	4.4	59.4
14	5.95	-15°	4.2	63.6
7	4.90	15°	4.1	67.8
13	5.95	0°	4.0	71.8
2	3.75	15°	3.7	75.5
4	3.75	-15°	3.1	78.6
15	5.95	-40°	2.7	81.3
9	4.90	-15°	2.6	83.9
10	4.90	-40°	2.6	86.5
18	7.58	0°	2.4	88.9
19	7.58	-15°	2.2	90.2
8	4.90	0°	1.9	93.0
3	3.75	0°	1.5	94.5
20	7.58	-40°	1.4	95.9
22	9.52	15°	1.3	97.2
23	9.52	0°	0.6	97.8

24	9.52	-15°	0.6	98.4
27	11.49	15°	0.6	99.0
21	9.52	40°	0.5	99.5
25	9.52	-40°	0.2	99.7
28	11.49	0°	0.1	99.8
29	11.49	-15°	0.1	99.9
26	11.49	40°	>0.1	99.9
30	11.49	-40°	>0.1	100.

Table 2 - Frequency of Occurrence of Wave Period and Direction Bins, Ranked from Most to Least Common.

III.A. WAVE TRANSFORMATION ANALYSIS - IDEALIZED CASE

This section is included to aid in understanding why an increase in channel depth will produce the changes in the wave parameters that it does. The bathymetry offshore of Sabine Pass, TX, is complicated by Sabine Bank and by the ship channel having several orientations along its length, and thus the wave refraction patterns can be difficult to interpret. Therefore, a few STWAVE runs were made with idealized bathymetry. These runs only modeled the portion of the channel seaward of Sabine Bank. The idealized grid was 18.6 by 18.6 miles (30 by 30 km) and had straight and parallel contours starting at a depth of 59 ft (18 m) at the seaward edge, rising to a depth of 33 ft (10 m), which is approximately the top of Sabine Bank. An 800 ft wide, 46 ft (14 m) deep channel (representing the existing channel) was cut into this bathymetry as shown in Figure 3.

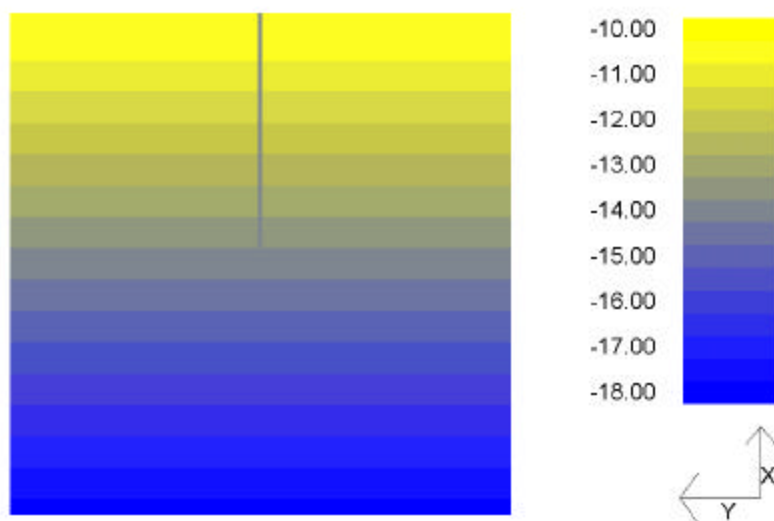


Figure 3 - Idealized bathymetry with 14 m deep channel.

All the waves used in these idealized examples had one meter heights and 10 second periods. These waves were transformed over this bathymetry (starting at the bottom, they propagated upward in the figure, toward land). For waves that traveled up the axis of the channel (zero incident wave angle), a symmetric pattern of wave refraction occurred. The waves tended to refract out of the channel, leading to reduced wave heights in the channel and broad lobes of slightly higher wave heights on each side of the channel. This is shown in Figure 4.

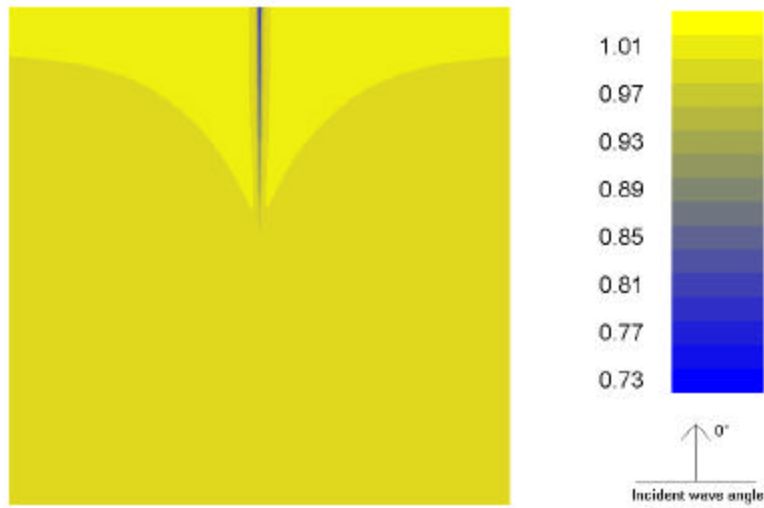


Figure 4 - Wave heights of a unit wave transformed over the bathymetry shown in Figure 3. Bright yellow shows areas of increased wave height, bright blue of decreased height. The scale at the right is wave height in meters.

A second idealized bathymetry grid was set up, which was identical to the first, except that it had a channel with a 56-foot (17 m) depth. This grid is shown in Figure 5.

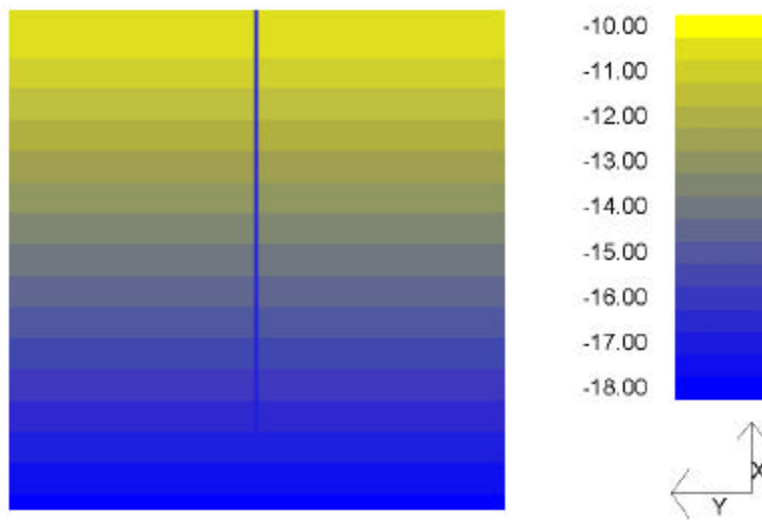


Figure 5 - Idealized bathymetry with a 17m deep channel.

Waves that were transformed up this deeper channel refracted (slightly) more strongly to both sides of the channel. The results, shown in figure 6, show a pattern similar to that seen in Figure 4 above, but with greater changes.

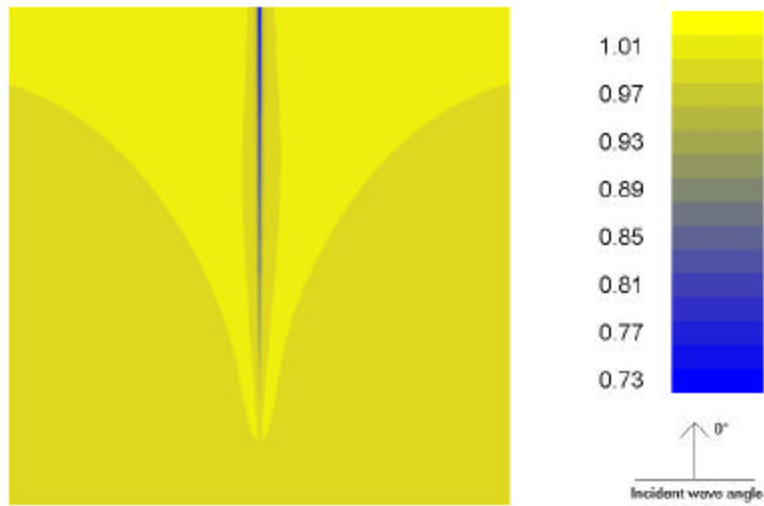


Figure 6 - Wave Heights of a Unit Wave Transformed over the Bathymetry Shown in Figure 5.

Figure 7 is a contour plot of the wave height differences between Figures 6 and 4. The wave height differences are the proposed (deeper channel) heights minus the existing conditions heights. This wave height difference plot shows that the proposed channel will yield lower wave heights in and immediately adjacent to the channel and broad lobes of slightly higher wave heights to the sides of the channel.

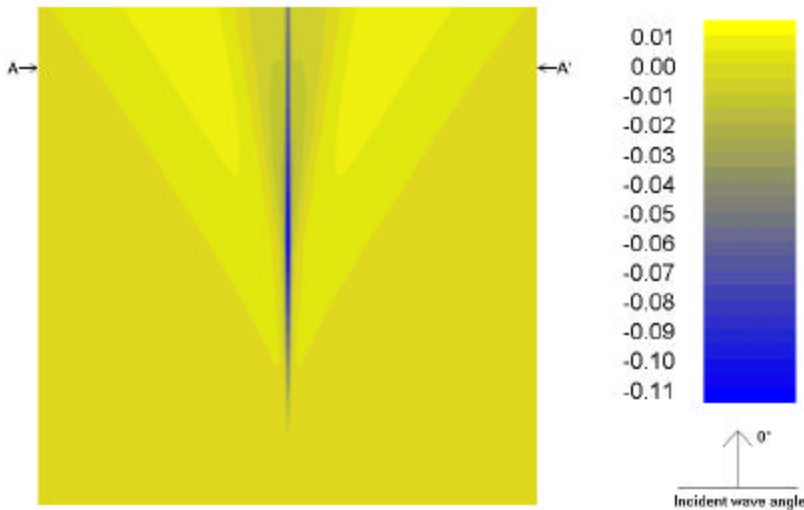


Figure 7 - Wave Height Difference Resulting from a Deeper Channel.

Figure 8 shows a cross-section of Figure 7 at the location A-A'. Note the decrease within the channel and the flat broad lobes out to each side. Also note that wave height differences are less than zero out to approximately 10 channel widths on each side of the channel.

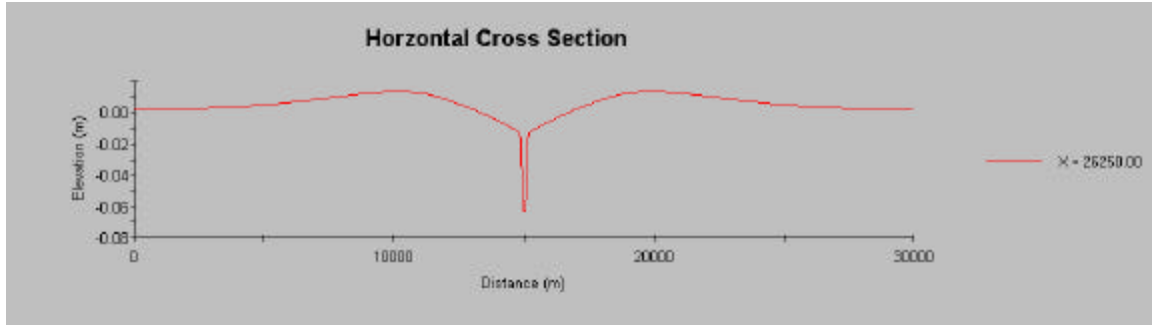


Figure 8 - Cross Section at A-A' in Figure 7.

In both channels, the waves bend (refract) away from the channel. In the deeper channel the refraction is greater. Figure 9 shows the wave angle changes (the proposed deeper channel minus the shallower channel). The proposed channel will cause waves to bend slightly more counter-clockwise on the left (west) side of the channel and slightly more clockwise on the right (east) side of the channel. In Figure 9 and in all wave angle difference figures, blue (negative numbers) represent a relative clockwise rotation of the wave crests and yellow (positive numbers) represent a relative counter-clockwise rotation of the wave crests.

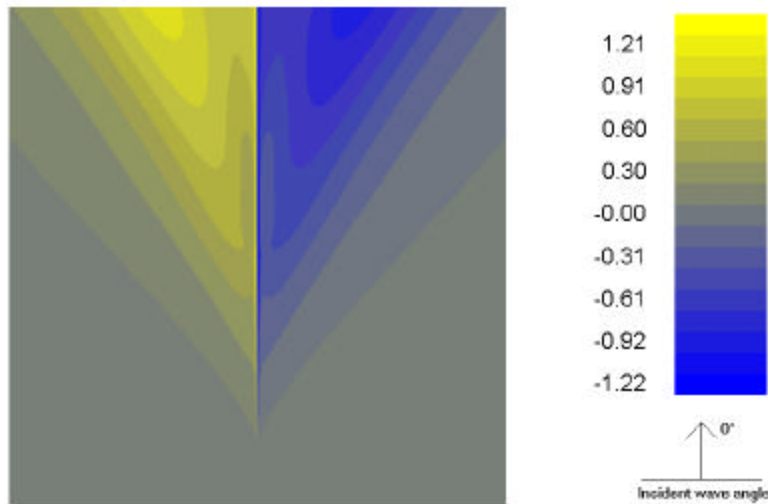


Figure 9 - Wave Angle Differences resulting from a Deeper Channel. The scale to the right is in degrees.

If the waves approach the channel at a non-zero angle, the symmetry in the results is lost. Wave height difference plots for waves approaching at 20° and 40° angles with respect to shore-normal (from the bottom right corner of the plots) are shown in Figures 10 and 11. On the up-wave side (to the right of the channel in these two figures) the lobe of higher wave heights is heightened and pressed against the right side of the channel. Though the greatest decrease in wave height is still within the channel, the trough of lower wave heights has spread out from the channel axis to the down-wave (left) side. The lobe of higher waves on the down-wave (left) side has diffused out to the point where it essentially no longer exists. This is the typical pattern

seen in the real bathymetry plots discussed in the sections below; increases in wave height on the up-wave side and decreases in wave height on the down-wave side of the channel.

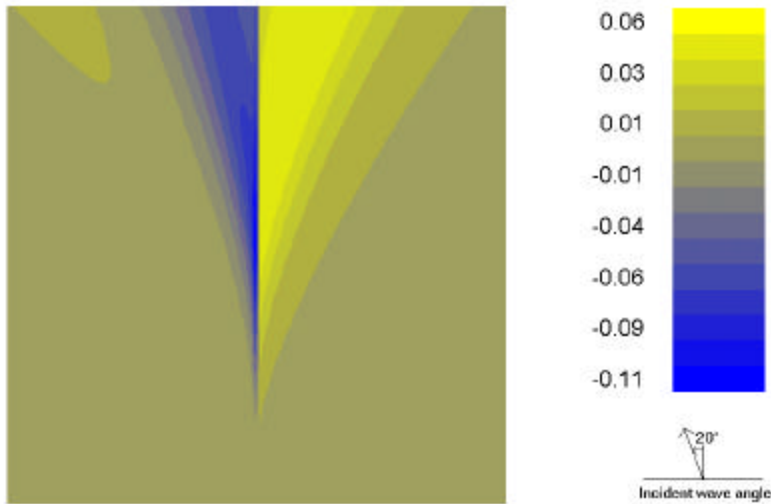


Figure 10 - Wave Height Differences for a 20° Incident Wave.

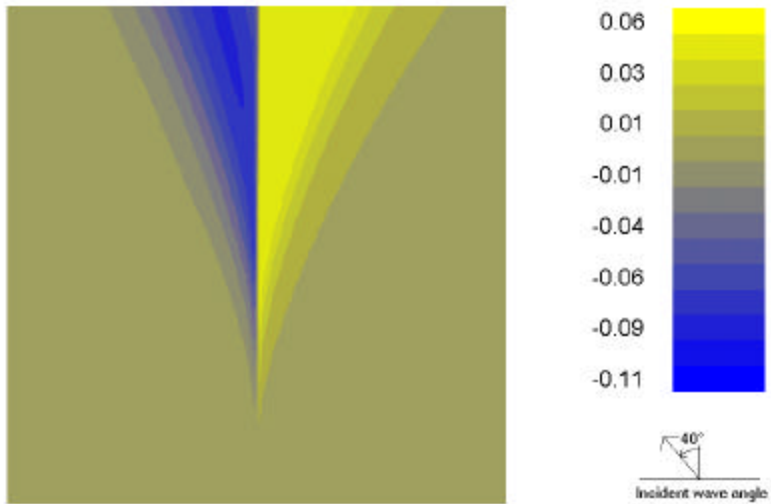


Figure 11 - Wave Height Differences for a 40° Incident Wave.

For oblique waves, the wave angle symmetry is also lost. The wave angle rotation away from the channel on the up-wave side is greater than on the down-wave side. This is shown in Figures 12 and 13.

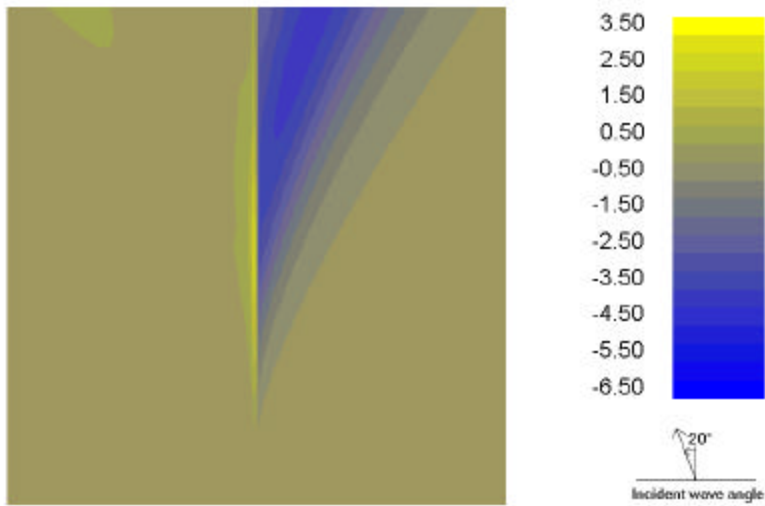


Figure 12 - Wave Angle Differences for a 20° Incident Wave.

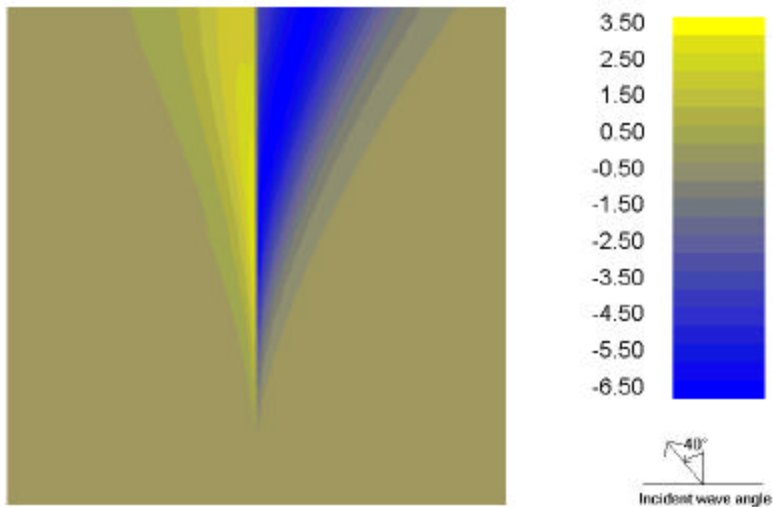


Figure 13 - Wave Angle Differences for a 40° Incident Wave.

These patterns can be seen in the results presented below where the more complicated, real bathymetry is used.

IIIB. WAVE TRANSFORMATION ANALYSIS - 50 FT CHANNEL

STWAVE wave-transformation simulations were performed for each of the 30 wave period / angle cases described in section IIB. First, a spectrum with a H_{m0} of 1 meter was generated for each of the 30 cases. These were used as input conditions for the STWAVE

simulation which transformed these spectra over the bathymetry shown in Figure 1B. The model takes into account refraction, shoaling, and dissipation and generates an output wave height and direction at each of the nearly 1 million cells in the grid. These wave simulations were run twice, first for the existing 40 ft channel conditions, and again for the proposed 50 ft channel conditions. Then, differences in the output for the two bathymetry conditions were compared. An example of these difference comparisons is shown in Figure 14.

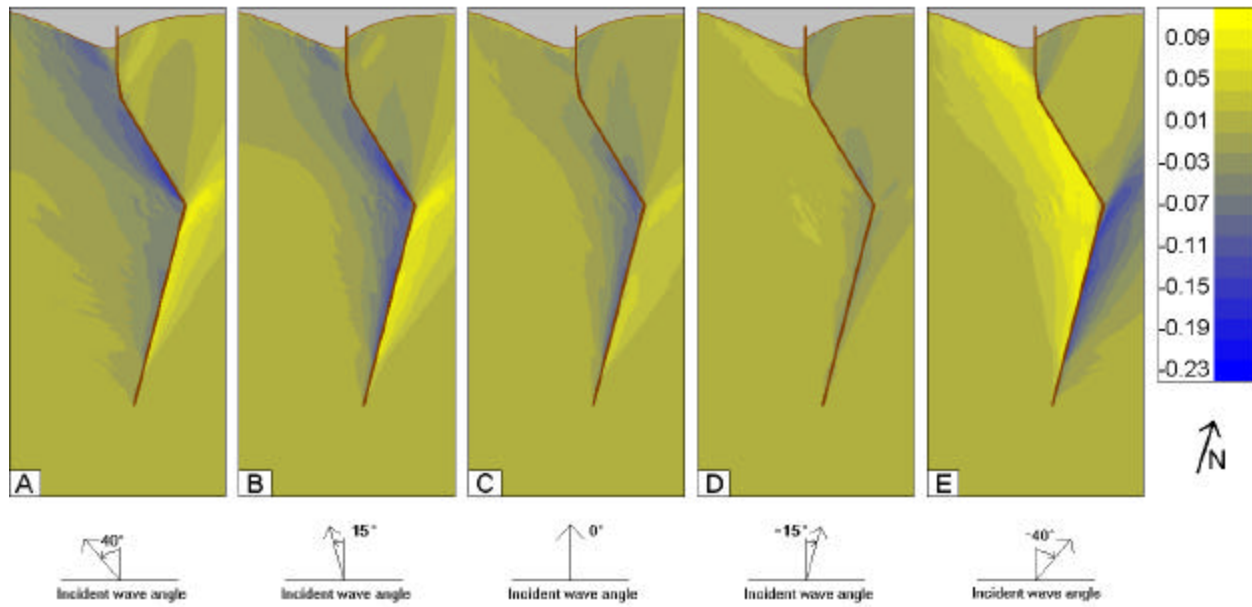


Figure 14 - Height Differences for 11.5 sec Period Waves; Cases 26-30, 50 ft Channel.

Figure 14 shows wave height differences (50 ft channel minus 40 ft channel) for 5 conditions (the 5 angle bands at the longest wave period, 11.49 seconds). Bright yellow areas are where the proposed channel will produce greater wave heights than the existing channel, and blue shows areas where the proposed channel will produce smaller wave heights. Regions of dark (muddy) yellow are regions of no change. The scale on the right can be considered as a percentage change from existing conditions. Seaward and to the sides of the tip of the proposed extension (at the bottom of the figures) the wave height changes are zero, as would be expected. Generally, wave heights are (slightly) increased on the sides of the channel that the waves are approaching from (the up-wave side) and are decreased on the down-wave side. Figure 14D shows nearly symmetrical wave height changes to the sides of the seaward leg of the channel, as discussed in section IIIA, as the direction of wave approach is approximately along the channel axis.

Long period waves are more strongly influenced by changes in the seafloor bathymetry than are short period waves. The wave conditions shown in Figure 14 are representative of the longest wave periods expected to occur in this region, and thus, this figure represents the extremes of the wave height changes that are expected to occur. The analysis of the 10-year hindcast of wave conditions described in section IIB shows that these conditions rarely occur. Combined, these 5 cases occur 1% of the time at this location in the Gulf of Mexico. Figure 15 shows wave height difference plots for 6.0-second period waves, conditions that occur much more commonly (approximately 37% of the time). These figures show smaller wave height

changes than in Figure 14. The rest of the wave height difference plots are shown in the appendix of this report (Figures A1-A6).

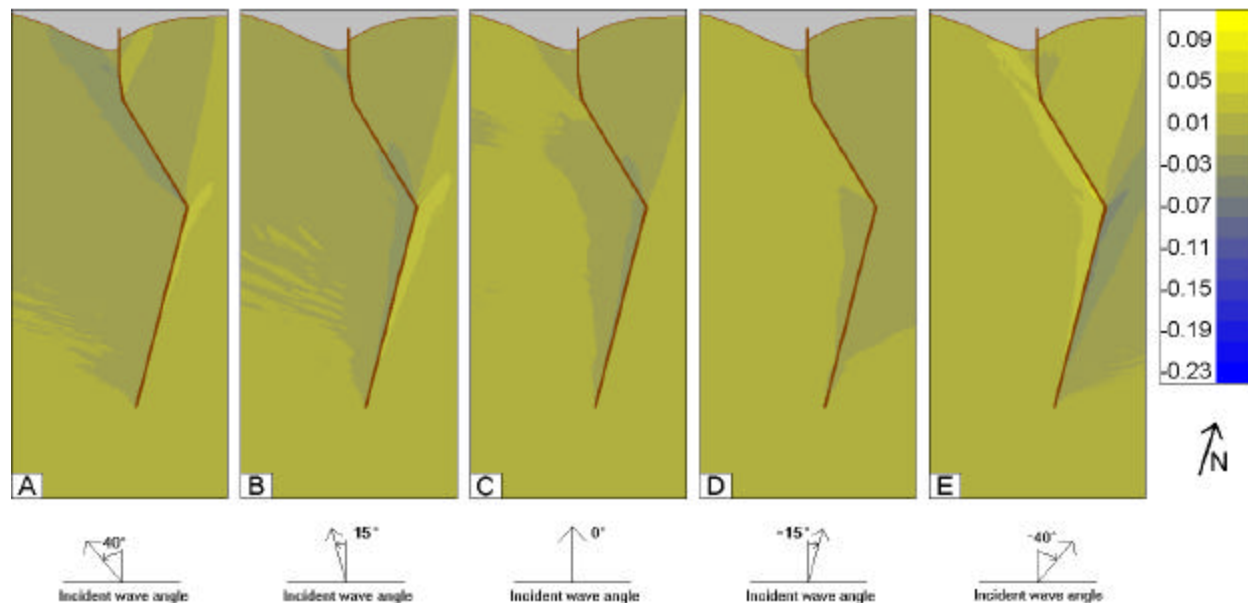


Figure 15 - Height Differences for 6.0 sec Period Waves; Cases 11-15, 50 ft Channel.

The height differences in Figure 15 show similar patterns to those shown in Figure 14, but smaller. Generally, wave heights increase on the up-wave sides and decrease on the down-wave sides. The other figures in the appendix all show this general pattern of increased wave heights on the up-wave side and decreased wave heights on the down-wave side. They also show decreasing differences as wave periods get smaller.

Table 3 lists the maximum wave height increases and decreases that occur for each of the 30 cases. While Figures A1-A6 show that for a majority of the times and locations, the change in wave height is essentially zero, Table 3 shows that the maximum possible changes are estimated to range from +12% to -22%. The maximum changes all occur offshore; the maximum increases are generally in the vicinity of Sabine Bank, and the maximum decreases occur within the ship channel. For most of the cases, and for all of the commonly occurring cases, the maximum height differences near the shoreline are usually $\pm 2\%$ or less. Waves approaching from the southwest (cases 5, 10, 15, 20, 25, and 30), which are uncommon, are the only ones that produce more than a 4% increase in height near the shoreline. These maximum height increases of up to 10% occur a few miles west of Sabine Pass. Cases 1, 6, 11, 16, 21, and 26 represent waves that approach at a strongly oblique angle from the east. These cause the greatest decrease in wave heights near the coast, up to 9%. Again, the region of maximum impact is a few miles west of Sabine Pass.

Case #	Wave period	Wave angle	% Occurrence	Shown in figure #	Change in Wave Height				
					% Max increase anywhere	% Max decrease anywhere	% Max decrease outside of channel	% Max increase near shore	% Max decrease near shore
1	3.75	40°	9.1	A1A	1	2	1	0	1
2	3.75	15°	3.7	A1B	1	2	1	0	0
3	3.75	0°	1.5	A1C	0	1	0	0	0
4	3.75	-15°	3.1	A1D	1	1	0	0	0
5	3.75	-40°	5.5	A1E	2	2	1	0	0
6	4.90	40°	9.3	A2A	4	5	3	0	2
7	4.90	15°	4.1	A2B	3	4	2	0	1
8	4.90	0°	1.9	A2C	1	3	1	0	1
9	4.90	-15°	2.6	A2D	2	3	1	1	0
10	4.90	-40°	2.6	A2E	5	4	3	1	0
11	5.95	40°	17.0	15A	6	8	4	0	3
12	5.95	15°	9.3	15B	5	8	3	0	2
13	5.95	0°	4.0	15C	2	6	3	0	2
14	5.95	-15°	4.2	15D	3	7	2	1	1
15	5.95	-40°	2.7	15E	8	7	5	2	0
16	7.58	40°	4.4	A4A	8	12	6	1	5
17	7.58	15°	4.7	A4B	7	13	7	0	3
18	7.58	0°	2.4	A4C	3	12	4	0	1
19	7.58	-15°	2.2	A4D	3	13	2	2	2
20	7.58	-40°	1.4	A4E	10	11	6	6	1
21	9.52	40°	0.5	A5A	10	16	9	1	7
22	9.52	15°	1.3	A5B	9	17	11	0	6
23	9.52	0°	0.6	A5C	4	17	6	0	4
24	9.52	-15°	0.6	A5D	3	18	5	2	4
25	9.52	-40°	0.2	A5E	11	16	10	8	1
26	11.49	40°	>0.1	14A	12	20	12	2	9
27	11.49	15°	0.6	14B	11	22	13	0	7
28	11.49	0°	0.1	14C	6	21	8	0	4
29	11.49	-15°	0.1	14D	4	23	5	4	4
30	11.49	-40°	>0.1	14E	12	20	12	10	2

Table 3 - Maximum Wave Height Differences for the 30 Different Wave Conditions; 50 ft Channel.

Along with wave height, wave angle near the shoreline is one of the parameters that influences sediment transport. In general, along the Sabine coast, a counter-clockwise change in the wave angle will increase the sediment transport that is moving in a westerly direction and decrease the eastward-directed transport. A clockwise change in the wave angle will do the opposite.

Figure 16 shows the changes in wave angle to be expected for 11.5-second waves if the 50 ft channel is constructed. It is the counterpart to Figure 14. Bright yellow areas (positive numbers) indicate where wave crests will be rotated in a counter-clockwise direction relative to their orientation with the existing conditions, blue (negative numbers) indicates areas of relative clockwise rotation, and muddy yellow-blue indicates areas of no relative rotation. Figure 16 shows wave angles generally being rotated away from the channel, with more pronounced rotation on the up-wave side.

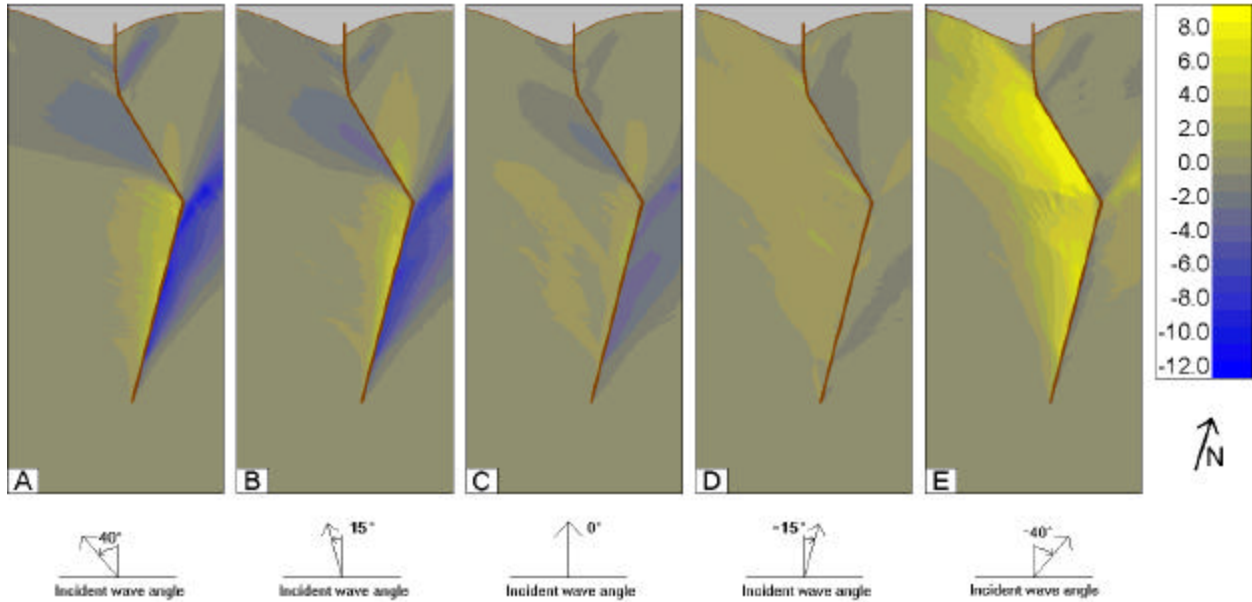


Figure 16 - Wave Angle Changes for 11.5 sec Period Waves; Cases 26-30, 50 ft Channel. The scale on the right hand side indicates the wave angle change in degrees.

The wave angle changes shown in Figure 16 are the most extreme to be expected, because they are representative of the longest wave periods in the wave climatology; and again, as shown in Section IIB, these conditions are relatively rare. Figure 17 shows wave angle difference plots for more common 6.0-second period waves, and is the counterpart to Figure 15.

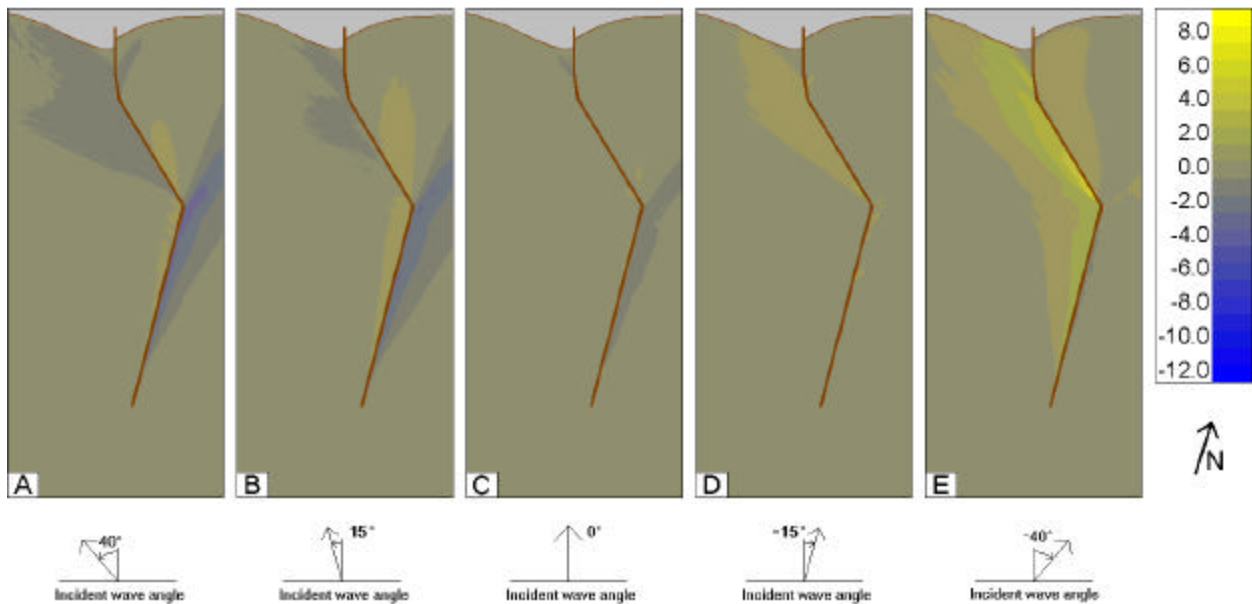


Figure 17 - Wave Angle Changes for 6.0 sec Period Waves; Cases 11-15, 50 ft Channel.

The rest of the wave angle difference plots are shown in the appendix of this report (Figures A7-A12). The wave angle changes shown in Figure 17 are similar to those in Figure

16, but considerably smaller. Wave angles are generally rotated away from the channel, with more pronounced rotation on the up-wave side. The other figures in the appendix all show this general pattern, and show decreasing angle changes as wave periods get smaller.

Table 4 lists the maximum changes in wave angle to be expected for each of the 30 cases, if the 50 ft channel is constructed. While Figures A7-A12 show that for a majority of the times and locations, the change in wave angle is essentially zero, Table 4 shows that the maximum possible changes are estimated to range from 10.5° counter-clockwise to 12.5° clockwise. These maximum angle changes occur offshore, generally in the vicinity of Sabine Bank. For most of the cases, and for all of the commonly occurring cases, the angle changes near the shoreline are usually 1° or less. Waves approaching obliquely from the southwest (cases 5, 10, 15, 20, 25, and 30) produce the greatest counter-clockwise wave angle changes near the shore of up to 5° in a region west of Sabine Pass. Waves approaching obliquely from the east (cases 1, 6, 11, 16, 21, and 26) cause the greatest clockwise change near the coast, of up to 2.6°.

Case #	Wave period	Wave angle	% Occurrence	Shown in figure #	Change in Wave Angle in Degrees			
					Max counter-clockwise change anywhere	Max clockwise change anywhere	Max counter-clockwise change near shore	Max clockwise change near shore
1	3.75	40°	9.1	A7A	0.7	0.6	0.3	0.1
2	3.75	15°	3.7	A7B	0.2	0.4	0.2	0.2
3	3.75	0°	1.5	A7C	0.4	0.3	0.1	0.1
4	3.75	-15°	3.1	A7D	0.6	0.2	0.1	0.0
5	3.75	-40°	5.5	A7E	1.2	0.4	0.4	0.0
6	4.90	40°	9.3	A8A	1.1	2.5	0.2	0.5
7	4.90	15°	4.1	A8B	1.1	1.8	0.2	0.3
8	4.90	0°	1.9	A8C	1.2	1.0	0.2	0.3
9	4.90	-15°	2.6	A8D	2.0	0.5	0.4	0.0
10	4.90	-40°	2.6	A8E	3.8	1.8	1.4	0.0
11	5.95	40°	17.0	17A	2.3	5.2	0.2	0.6
12	5.95	15°	9.3	17B	2.6	3.7	0.3	0.6
13	5.95	0°	4.0	17C	2.4	2.2	0.2	0.5
14	5.95	-15°	4.2	17D	2.6	1.4	0.6	0.2
15	5.95	-40°	2.7	17E	7.0	2.9	2.3	0.0
16	7.58	40°	4.4	A10A	4.0	8.3	0.2	1.0
17	7.58	15°	4.7	A10B	4.6	5.8	0.2	1.1
18	7.58	0°	2.4	A10C	3.9	3.6	0.2	0.8
19	7.58	-15°	2.2	A10D	2.8	2.7	0.8	0.5
20	7.58	-40°	1.4	A10E	9.6	4.4	3.2	0.0
21	9.52	40°	0.5	A11A	5.1	10.6	0.4	2.1
22	9.52	15°	1.3	A11B	6.3	7.4	0.4	1.4
23	9.52	0°	0.6	A11C	5.1	4.7	0.2	1.0
24	9.52	-15°	0.6	A11D	3.6	3.8	0.8	0.5
25	9.52	-40°	0.2	A11E	10.3	5.6	4.3	0.2
26	11.49	40°	>0.1	16A	6.5	12.5	0.5	2.6
27	11.49	15°	0.6	16B	7.8	8.8	0.3	1.6
28	11.49	0°	0.1	16C	6.1	5.4	0.5	1.0
29	11.49	-15°	0.1	16D	4.7	4.5	1.0	0.6
30	11.49	-40°	>0.1	16E	10.5	6.5	5.0	0.4

Table 4 - Maximum Wave Angle Differences for the 30 Different Wave Conditions; 50 ft Channel.

Figures 18 and 19 give the wave height and angle changes for the five most frequently occurring wave cases. Combined, these five cases represent wave conditions that occur over half of the time. (See Table 2.) These five cases all show zero change or decreased wave heights

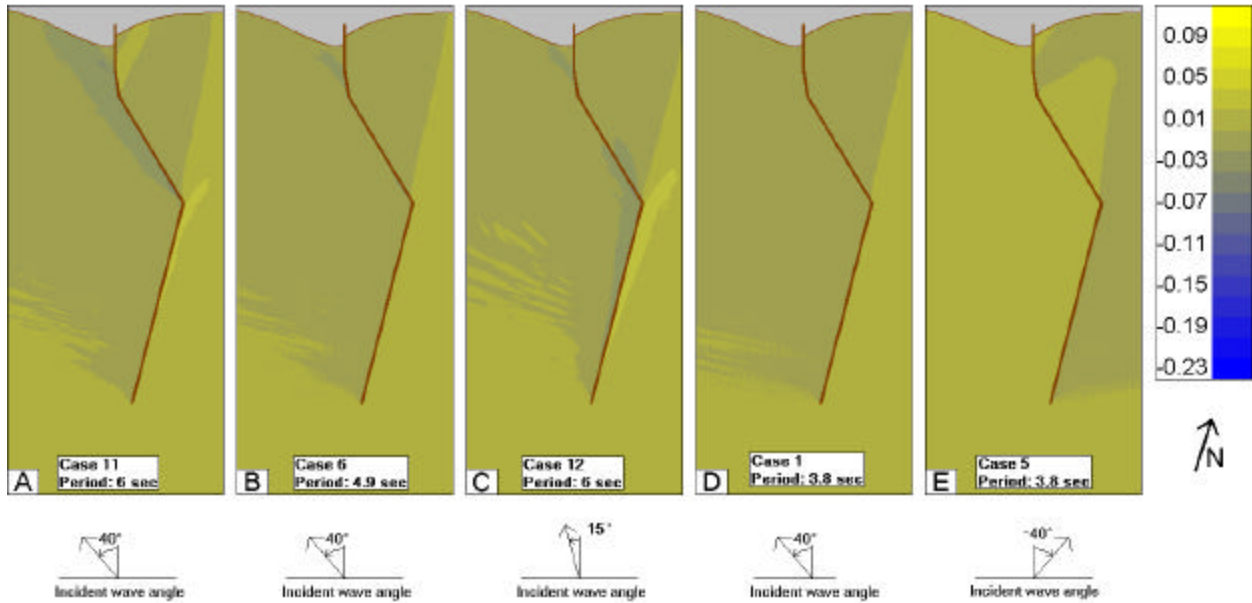


Figure 18 - Five Most Common Wave Height Difference Plots; 50 ft Channel. Case 11 - 17.0%, Case 6 - 9.3%, Case 12 - 9.3%, Case 1 - 9.1%, Case 5 - 5.5%. Together, these five cases represent 50.3% of wave conditions.

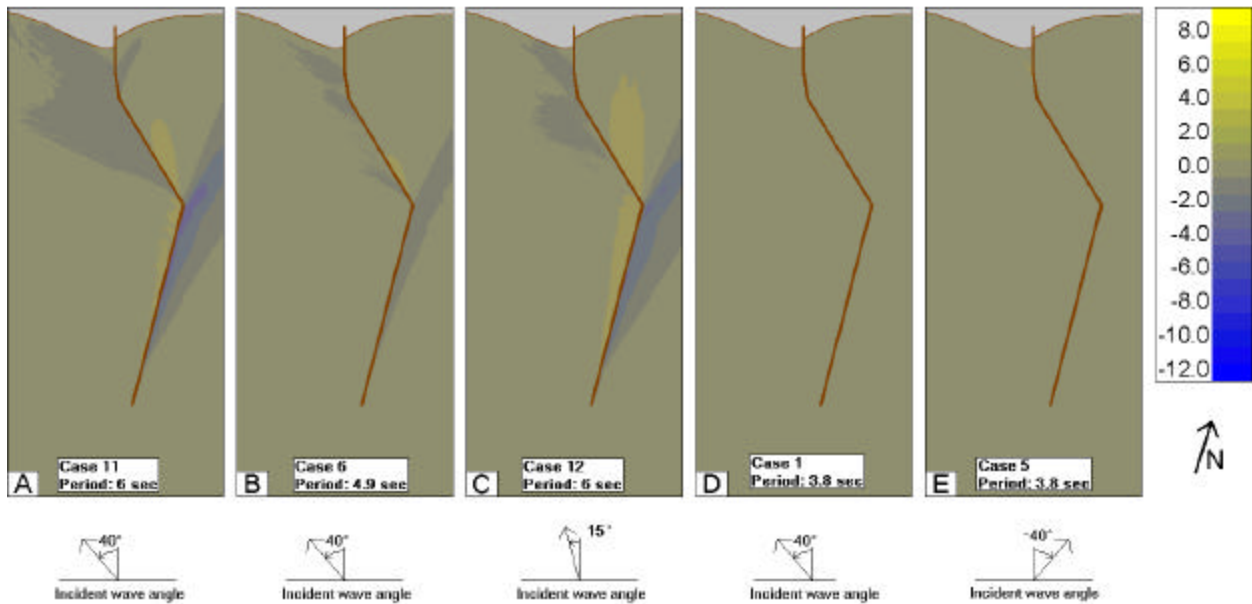


Figure 19 - Five Most Common Wave Angle Change Plots; 50 ft Channel.

near the shoreline, with the decrease being perhaps a little greater to the west of Sabine Pass. These cases show a degree or less of clockwise change in the wave angle at the shoreline west of Sabine Pass, and essentially no change in wave angle along the shore east of Sabine Pass.

IIIC. SHORELINE CHANGE ANALYSIS - 50 FT CHANNEL

Wave parameters near the shoreline, which were computed by STWAVE, were used as input to the shoreline change model, GENESIS. This model estimated longshore sediment transport quantities and shoreline changes throughout the 10-year simulation interval, 1990-1999. GENESIS simulations were run using both sets of STWAVE outputs; those generated using the existing bathymetry and those generated using the proposed 50 ft channel bathymetry. Results of these simulations were used to estimate the average annual rate of shoreline change and the average annual longshore sand transport rate along the 20 miles of shoreline centered at Sabine Pass.

The top plot in Figure 20 shows the estimated net longshore transport rate around Sabine Pass for the proposed 50 ft channel and for existing conditions. The net rate is to the west all along this coastline except for the three miles immediately east of Sabine Pass. At the scale of this plot, the transport rates for the existing conditions and for the proposed 50 ft channel essentially fall on top of each other. The lower plot in Figure 20 shows the estimated change in the net transport rate if the 50 ft channel were constructed. It is the difference in the two lines in the top plot. This plot shows that west of Sabine Pass, the net westward transport would be slightly reduced (by a maximum of about 2800 yds³/yr near the jetties). In the first two miles east of Sabine Pass, the net eastward transport would also be slightly reduced (by a maximum of about 1400 yds³/yr), and further east there would be essentially no change.

Figure 21 shows the estimated rate of shoreline change. The top plot in Figure 21 indicates erosion within a half mile on either side of the Sabine jetties, with only smaller fluctuations elsewhere. Again, at the scale of this plot, it is difficult to see any differences in the proposed and existing conditions. The bottom plot in Figure 21 shows the difference between the two lines in the top plot. It is the estimated change in the shoreline change rate if the 50 ft channel were built. This plot shows that the erosion adjacent to both sides of the jetties would be reduced. Between a half mile and 3-4 miles on either side of the jetties the erosion would be increased (or the accretion decreased) by less than 0.5 ft/yr, and further from the jetties than that, the change in the shoreline change would decrease to zero.

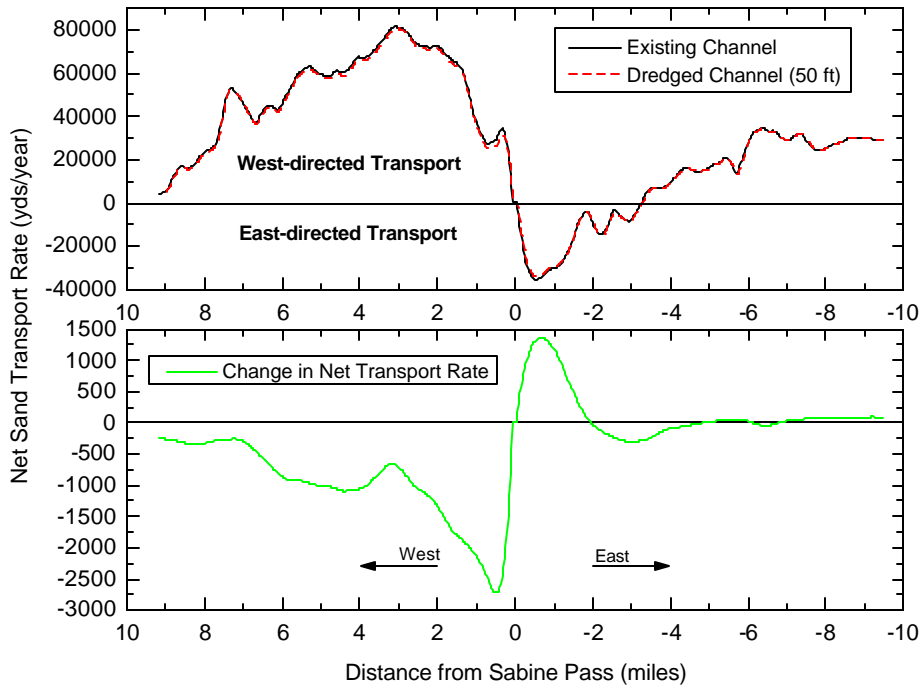


Figure 20 - Net Estimated Annual Sand Transport Rate - 50 ft Channel.

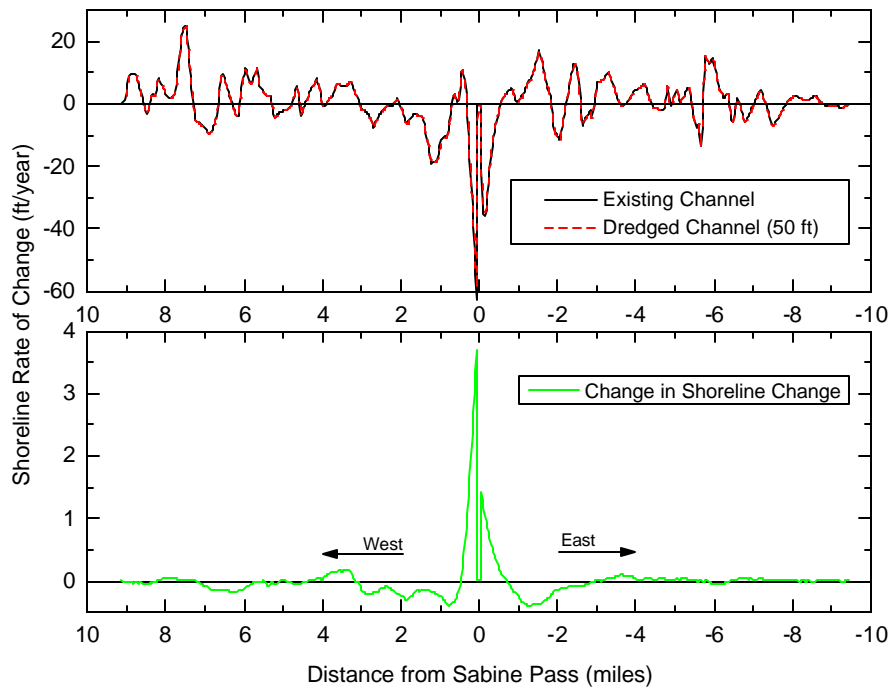


Figure 21 – Net Estimated Annual Rate of Shoreline Change - 50 ft Channel.

IIID. WAVE TRANSFORMATION ANALYSIS - 45 FT CHANNEL

STWAVE near shore wave-transformation simulations were performed using the proposed 45 ft channel bathymetry. These output wave conditions were compared to the STWAVE output using existing bathymetry. Contour plots of wave height differences and wave angle changes are given in the Appendix (Figures A13-A18, and A19-A24, respectively) for all 30 cases. The contour range and step intervals in Figures A13-A24 are reduced as compared to Figures A1-A12 in order to illustrate the considerably smaller wave differences caused by the 45 ft channel alternative compared to those caused by the 50 ft channel.

Table 5 lists the maximum wave height increases and decreases for each of the 30 wave cases (45 ft channel minus existing 40 ft channel). For all cases these height changes are less

Case #	Wave period	Wave angle	% Occurrence	Shown in figure #	Change in Wave Height				
					% Max increase anywhere	% Max decrease anywhere	% Max decrease outside of channel	% Max increase near shore	% Max decrease near shore
1	3.75	40°	9.1	A13A	1	1	1	0	0
2	3.75	15°	3.7	A13B	1	1	0	0	0
3	3.75	0°	1.5	A13C	0	1	0	0	0
4	3.75	-15°	3.1	A13D	1	1	0	0	0
5	3.75	-40°	5.5	A13E	2	1	0	0	0
6	4.90	40°	9.3	A14A	3	3	2	0	1
7	4.90	15°	4.1	A14B	2	2	1	0	1
8	4.90	0°	1.9	A14C	1	2	1	0	0
9	4.90	-15°	2.6	A14D	2	3	1	0	0
10	4.90	-40°	2.6	A14E	3	3	1	1	0
11	5.95	40°	17.0	A15A	4	5	3	0	2
12	5.95	15°	9.3	A15B	4	5	2	0	1
13	5.95	0°	4.0	A15C	1	5	2	0	1
14	5.95	-15°	4.2	A15D	2	6	2	1	1
15	5.95	-40°	2.7	A15E	5	5	2	1	0
16	7.58	40°	4.4	A16A	6	7	3	1	2
17	7.58	15°	4.7	A16B	5	9	5	0	2
18	7.58	0°	2.4	A16C	2	9	3	0	1
19	7.58	-15°	2.2	A16D	2	10	2	1	1
20	7.58	-40°	1.4	A16E	6	8	4	3	0
21	9.52	40°	0.5	A17A	7	10	6	1	4
22	9.52	15°	1.3	A17B	7	12	7	0	3
23	9.52	0°	0.6	A17C	3	13	3	0	2
24	9.52	-15°	0.6	A17D	2	14	3	1	2
25	9.52	-40°	0.2	A17E	8	12	6	4	1
26	11.49	40°	>0.1	A18A	9	13	7	2	5
27	11.49	15°	0.6	A18B	8	15	8	0	4
28	11.49	0°	0.1	A18C	4	16	7	0	2
29	11.49	-15°	0.1	A18D	3	18	3	2	2
30	11.49	-40°	>0.1	A18E	8	15	8	5	1

Table 5 - Maximum Wave Height Differences for the 30 Different Wave Conditions; 45 ft Channel.

than or equal to those shown in Table 3 (the 50 ft channel alternative), though the patterns of wave height changes are quite similar (compare Figures A13-A18 with A1-A6). The maximum wave height changes, which all occur offshore, are estimated to range from +9% to -18%. Near shore the wave height differences are usually $\pm 1\%$ or less. The maximum wave height increases, of up to 5%, occur a few miles west of Sabine Pass and are produced by waves approaching obliquely from the southwest. The maximum wave height decreases, also of up to 5% and also impacting the coast west of Sabine Pass, are produced by waves approaching obliquely from the east.

Table 6 lists the maximum changes in wave angle to be expected for each of the 30 cases, if the 45 ft channel is constructed. Again, all of the maximum wave angle changes are less than or equal to those shown in Table 4 (the 50 ft channel alternative), though the patterns of wave angle changes are quite similar (compare Figures A19-A24 with A7-A12). The maximum angle changes are estimated to range from 7.1° counter-clockwise to 9.2° clockwise. Near the

Case #	Wave period	Wave angle	% Occurrence	Shown in figure #	Change in Wave Angle in Degrees			
					Max counter-clockwise change anywhere	Max clockwise change anywhere	Max counter-clockwise change near shore	Max clockwise change near shore
1	3.75	40°	9.1	A19A	0.5	0.5	0.1	0.1
2	3.75	15°	3.7	A19B	0.2	0.3	0.1	0.1
3	3.75	0°	1.5	A19C	0.3	0.2	0.1	0.0
4	3.75	-15°	3.1	A19D	0.4	0.2	0.1	0.0
5	3.75	-40°	5.5	A19E	0.8	0.4	0.1	0.0
6	4.90	40°	9.3	A20A	0.9	1.8	0.1	0.2
7	4.90	15°	4.1	A20B	0.9	1.3	0.1	0.2
8	4.90	0°	1.9	A20C	0.9	0.8	0.1	0.0
9	4.90	-15°	2.6	A20D	1.3	0.4	0.2	0.0
10	4.90	-40°	2.6	A20E	2.3	1.3	0.5	0.0
11	5.95	40°	17.0	A21A	1.7	3.7	0.1	0.4
12	5.95	15°	9.3	A21B	2.0	2.7	0.2	0.4
13	5.95	0°	4.0	A21C	1.8	1.9	0.1	0.1
14	5.95	-15°	4.2	A21D	1.7	1.3	0.4	0.1
15	5.95	-40°	2.7	A21E	4.3	2.4	1.1	0.0
16	7.58	40°	4.4	A22A	2.6	6.0	0.1	0.9
17	7.58	15°	4.7	A22B	3.6	4.3	0.1	0.8
18	7.58	0°	2.4	A22C	3.9	3.1	0.2	0.5
19	7.58	-15°	2.2	A22D	1.8	2.7	0.5	0.3
20	7.58	-40°	1.4	A22E	6.0	3.6	1.5	0.0
21	9.52	40°	0.5	A23A	3.4	7.8	0.1	1.3
22	9.52	15°	1.3	A23B	4.8	5.5	0.1	0.9
23	9.52	0°	0.6	A23C	3.8	3.9	0.2	0.6
24	9.52	-15°	0.6	A23D	2.5	3.5	0.4	0.4
25	9.52	-40°	0.2	A23E	6.9	4.4	1.8	0.2
26	11.49	40°	>0.1	A24A	4.5	9.2	0.1	2.0
27	11.49	15°	0.6	A24B	5.8	6.4	0.1	1.1
28	11.49	0°	0.1	A24C	4.6	4.6	0.3	0.7
29	11.49	-15°	0.1	A24D	3.1	4.2	0.6	0.5
30	11.49	-40°	>0.1	A24E	7.1	5.2	2.4	0.3

Table 6 - Maximum Wave Angle Differences for the 30 Different Wave Conditions; 45 ft Channel.

shoreline, the wave angle changes are usually less than $\pm 0.5^\circ$. The maximum near shore wave angle changes, of up to 2.4° , are produced by strongly oblique waves.

III. SHORELINE CHANGE ANALYSIS - 45 FT CHANNEL

GENESIS simulations were performed using the STWAVE output that was generated using the proposed 45 ft channel bathymetry. The GENESIS model produced longshore sediment transport amounts and shoreline changes throughout the 10-year simulation interval, 1990-1999, as had been done previously for the proposed 50 ft channel and for existing conditions. Results of these simulations were used to estimate the average annual longshore sand transport rate and the average annual rate of shoreline change. Figures 22 and 23 show that the change in the sediment transport rate and the change in the shoreline change rate for the 45 ft alternative would be about half that for the 50 ft alternative (compare Figures 22 and 23 with 20 and 21).

The top plot in Figure 22 shows the net predicted longshore transport rate around Sabine Pass for both the proposed 45 ft channel and for existing conditions. This top figure is essentially identical to the top plot in Figure 20. The lower plot in Figure 22 shows the estimated change in the net transport rate if the 45 ft channel were constructed. It is the difference in the two lines in the top plot. This plot shows a curve that has essentially the same shape as in the lower plot of Figure 20, but the amplitude is reduced by about half. Thus, the 45 ft alternative is expected to produce about half the changes in transport rate that the 50 ft channel would; the maximum would be a reduction of the net westward transport just west of the jetties of about $1500 \text{ yds}^3/\text{yr}$.

Figure 23 shows the estimated rate of shoreline change. The top plot in Figure 23 shows a prediction of erosion within a half mile on either side of the Sabine jetties, with only smaller fluctuations elsewhere. This top figure is essentially identical to the top plot in Figure 22. The bottom plot in Figure 23 shows the difference between the two lines in the top plot. It is the estimated change in the shoreline change rate if the 45 ft channel is constructed. This plot is similar in shape to the bottom plot in Figure 21, but again, the amplitude is reduced by about half. This plot shows that the erosion adjacent to both sides of the jetties would be reduced by up to about two feet per year. Between a half-mile and 3 miles on either side of the jetties it is predicted that the erosion would be increased (or the accretion decreased) by less than 0.3 ft/yr , and further from the jetties than that, the change in the shoreline change rate would decrease to zero.

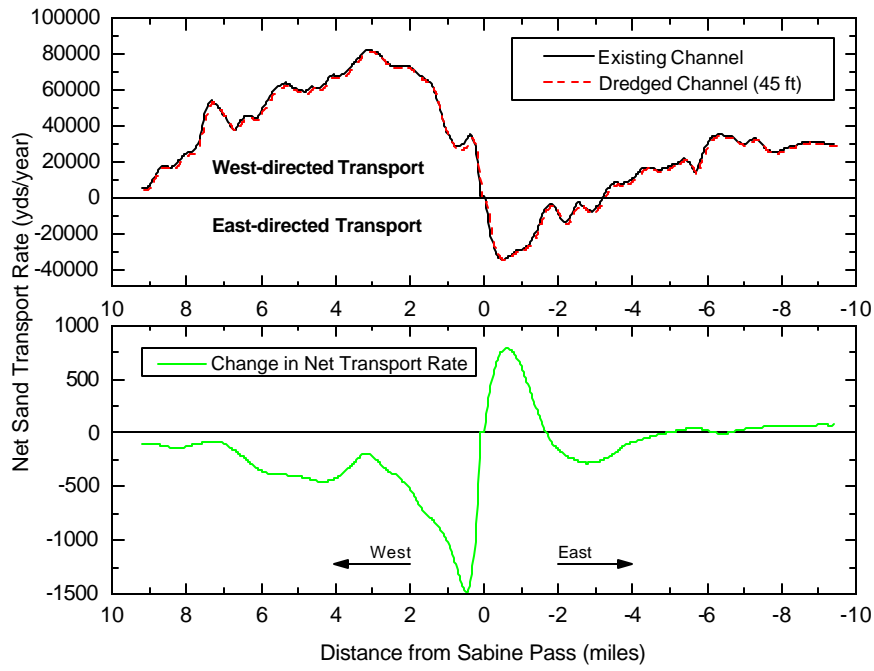


Figure 22 - Net Estimated Annual Sand Transport Rate - 45 ft Channel.

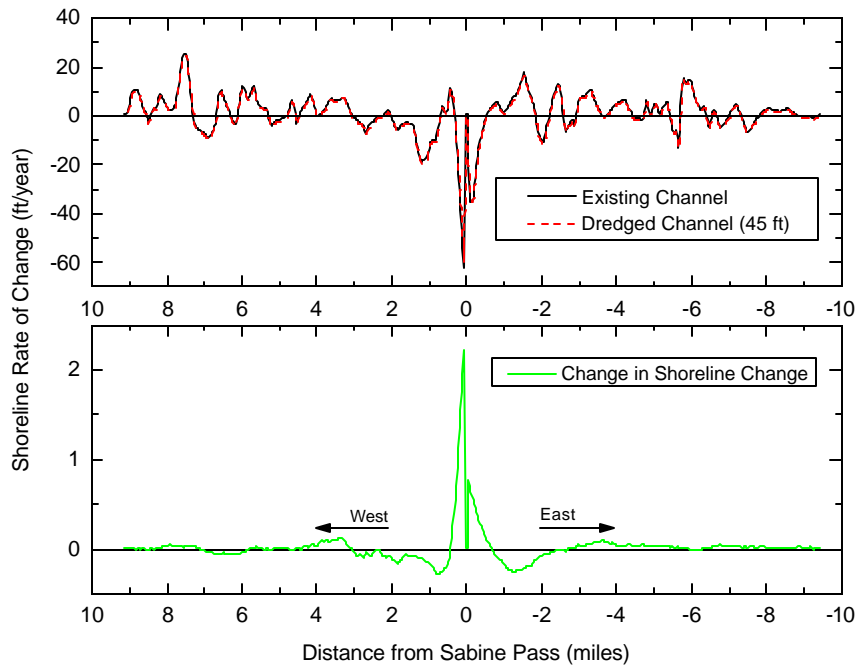


Figure 23 – Net Estimated Annual Rate of Shoreline Change - 45 ft Channel.

IV. CONCLUSIONS

- For all of the project design alternatives, the largest predicted impact on the shoreline will be the beneficial reduction of erosion within a half mile of the Sabine jetties.
- For all of the design alternatives, some changes in the existing average annual net longshore sediment transport rate are expected. These will be mostly confined to a region of approximately 3 to 4 miles on either side of the Sabine Pass jetties. West of the jetties the net westward transport will be decreased, and east of the jetties the net eastward transport rate will be decreased.
- Construction of the 50 ft channel design alternative is expected to result in wave height changes near the shore ranging from extremes of -9% to +10%, with typical values ranging from -3% to +2%. These numbers represent the maximum predicted changes anywhere along the shore for various offshore wave conditions, not the average changes along the entire length of shoreline. These maximum changes will generally occur within 3-4 miles of the Sabine jetties. Typical near shore wave angle changes are predicted to be less than 1.0° .
- For the 50 ft channel design alternative, the rate of shoreline erosion within a half mile on either side of the jetties is expected to decrease by up to 3.5 ft/yr. Between a half mile and 3-4 miles from the jetties, the project-induced changes in the present shoreline erosion and accretion rates are predicted to be no more than 4-6 inches a year. Further than 3-4 miles from the jetties, the project-induced shoreline impacts are predicted to essentially diminish to zero.
- Construction of the 45 ft channel design alternative is expected to result in wave height changes near the shore ranging from extremes of -8% to +9%, with typical values ranging from -2% to +1%. Again, these are the maximum, not average predicted changes. These values will generally occur within 3-4 miles of the Sabine jetties. Typical near shore wave angle changes are predicted to be less than 0.5° .
- For the 45 ft design alternative, the rate of shoreline erosion within a half mile on either side of the jetties is expected to decrease by up to 2 ft/yr. Between a half mile and 3-4 miles from the jetties, the project-induced changes in the present shoreline erosion and accretion rates are predicted to be no more than 2-4 inches a year. Further than 3-4 miles from the jetties, the project-induced shoreline impacts are predicted to essentially diminish to zero.
- Construction of the 48 ft channel alternative is expected to produce shoreline impacts that are greater than those found for the 45 ft channel and less than those found for the 50 ft channel.
- A navigation benefit of reduced wave heights within the channel of typically 2 to 10% is anticipated, with the larger percentage reductions generally occurring during times of bigger waves.

APPENDIX

Some figures presented in the main text are repeated here for ease of comparison. Figures A1-A6 are height difference plots for the 50 ft channel compared to the existing channel. Periods increase from A1 to A6. Figures A7 - A12 are the corresponding wave angle difference plots. Figures A13 - A24 are the height (A13-A18) and angle (A19-A24) difference plots comparing the 45 ft channel to the existing channel.

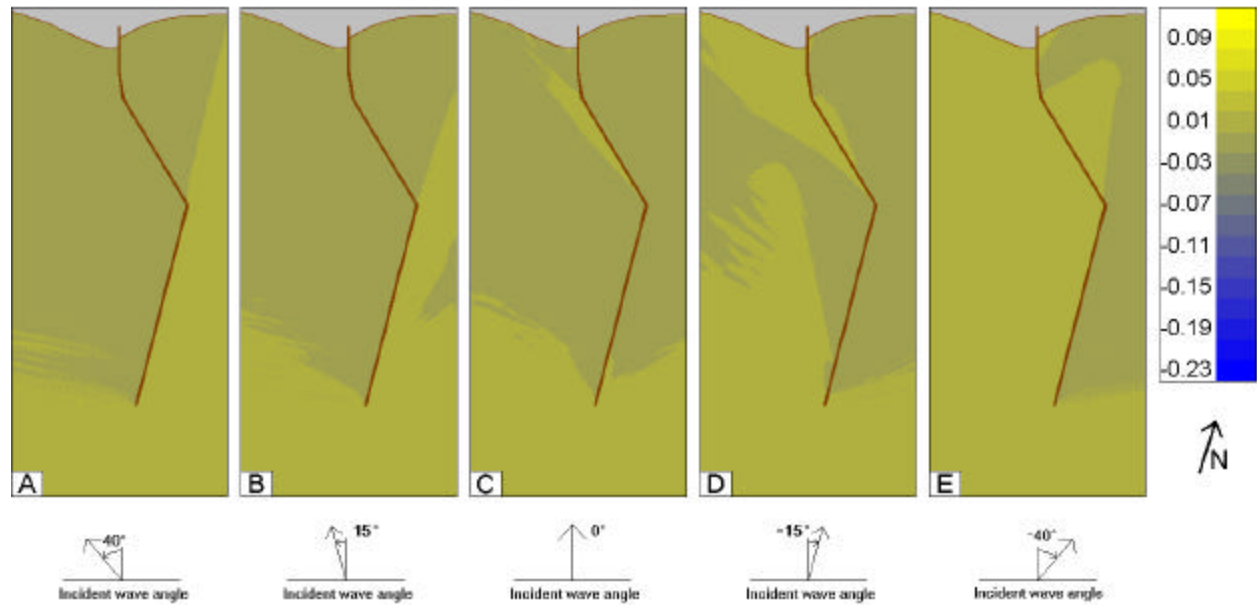


Figure A 1 - Height Differences for 50 ft vs. Existing Channel for 3.8 sec Period Waves, Cases 1-5.

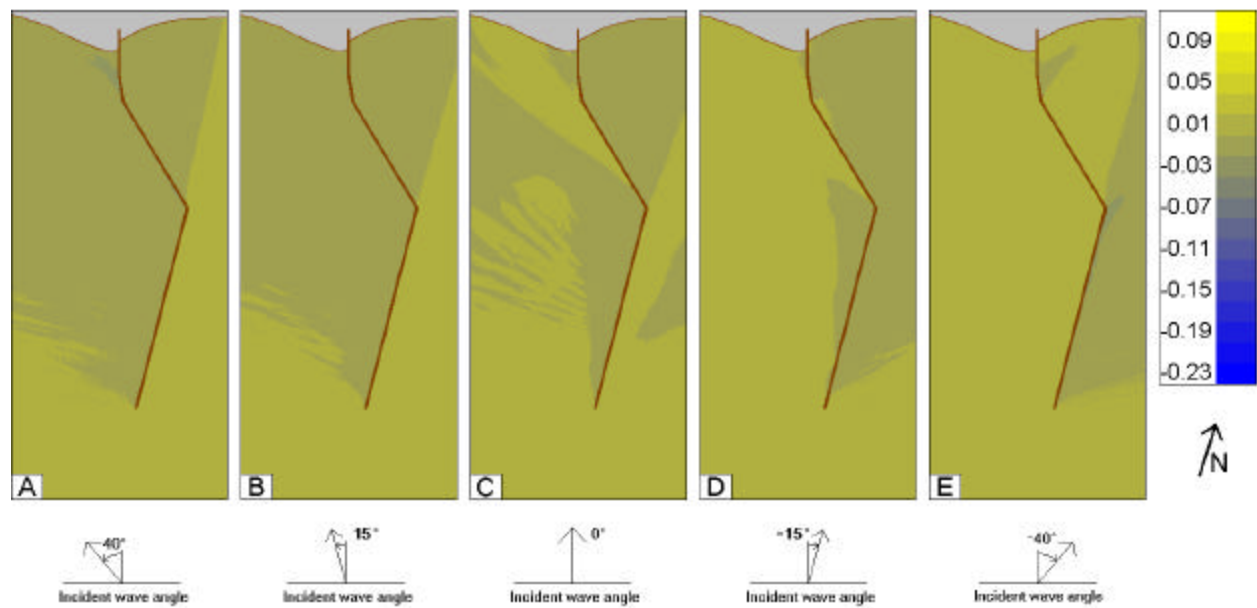


Figure A 2 - Height Differences for 50 ft vs. Existing Channel for 4.9 sec Period Waves, Cases 6-10.

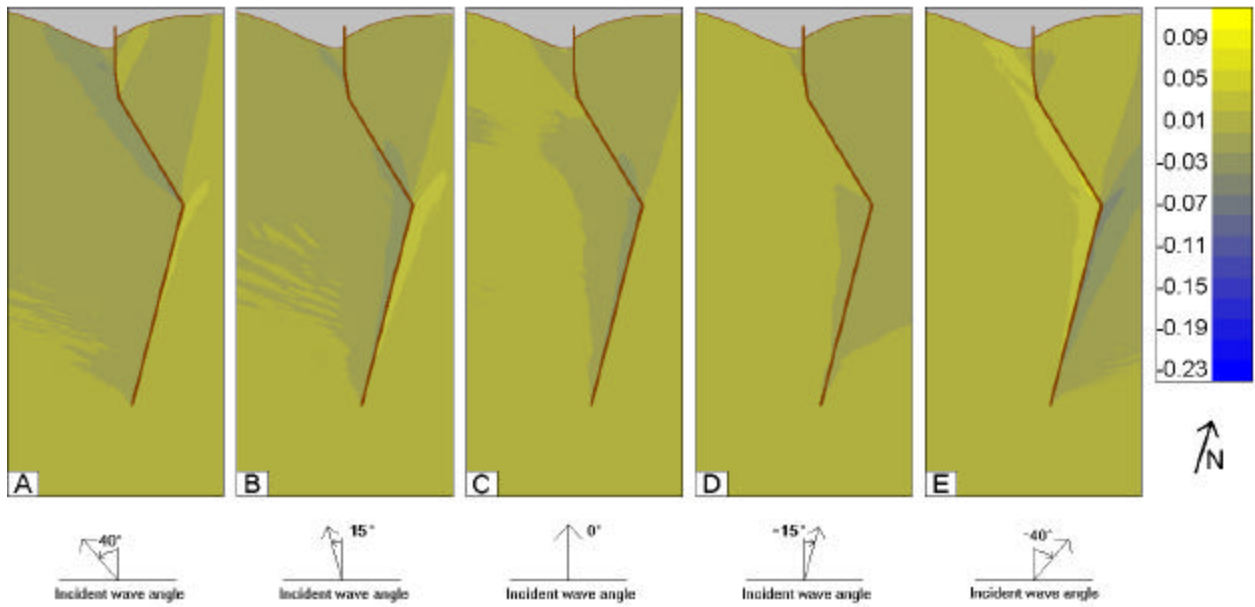


Figure A 3 - Height Differences for 50 ft vs. Existing Channel for 6.0 sec Period Waves, Cases 11-15.

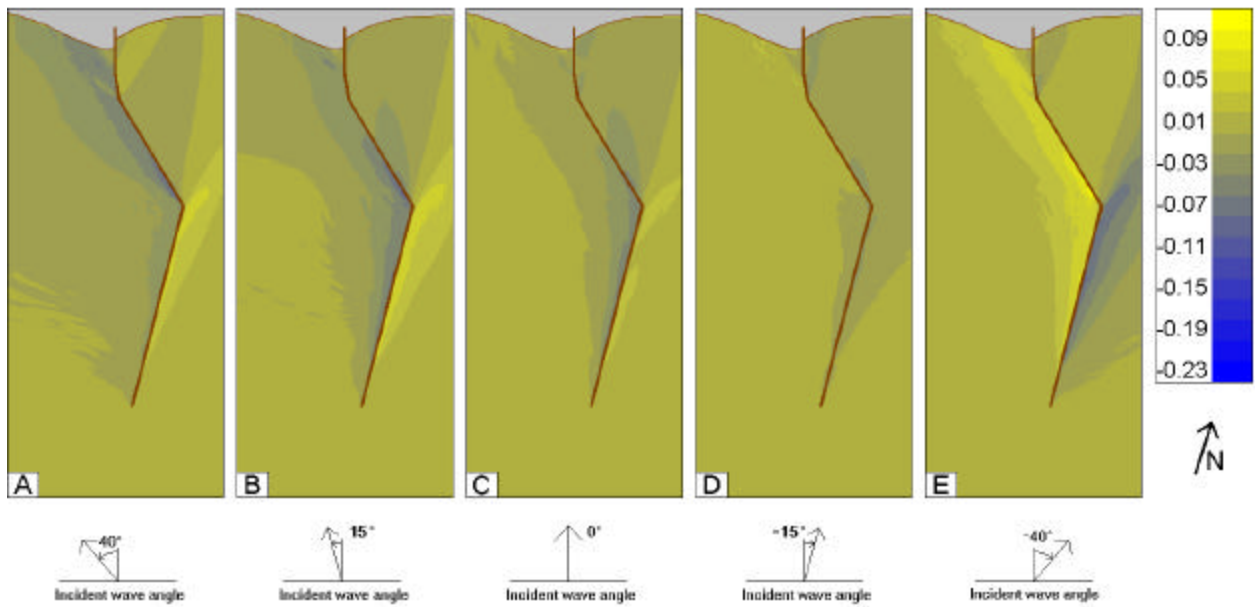


Figure A 4 - Height Differences for 50 ft vs. Existing Channel for 7.6 sec Period Waves, Cases 16-20.

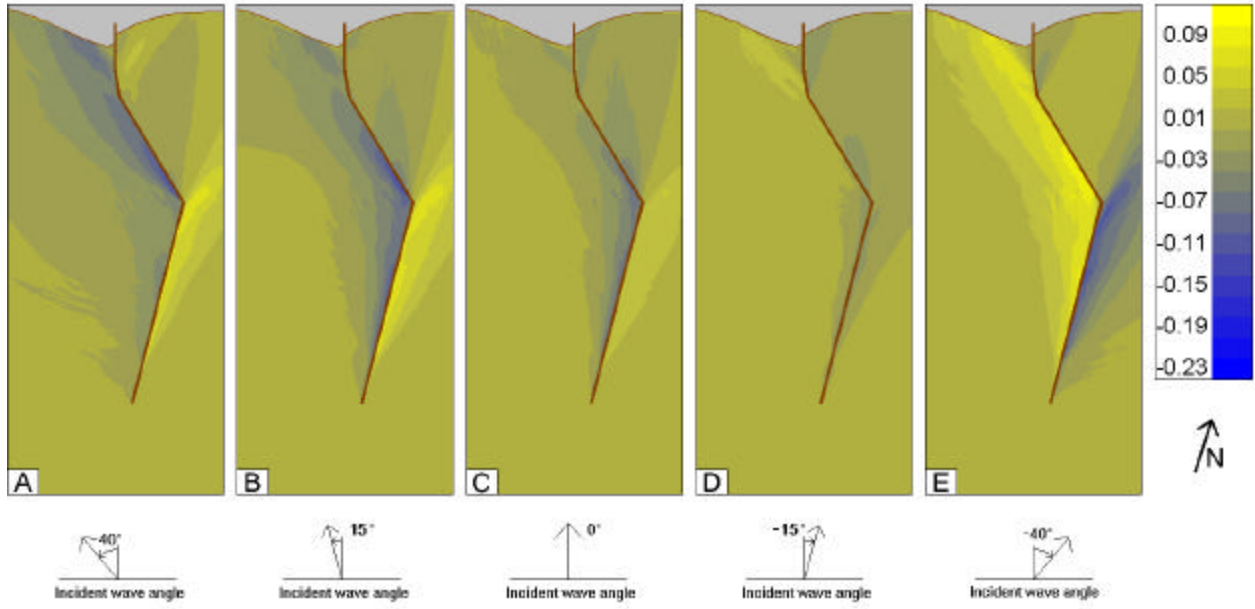


Figure A 5 - Height Differences for 50 ft vs. Existing Channel for 9.5 sec Period Waves, Cases 21-25.

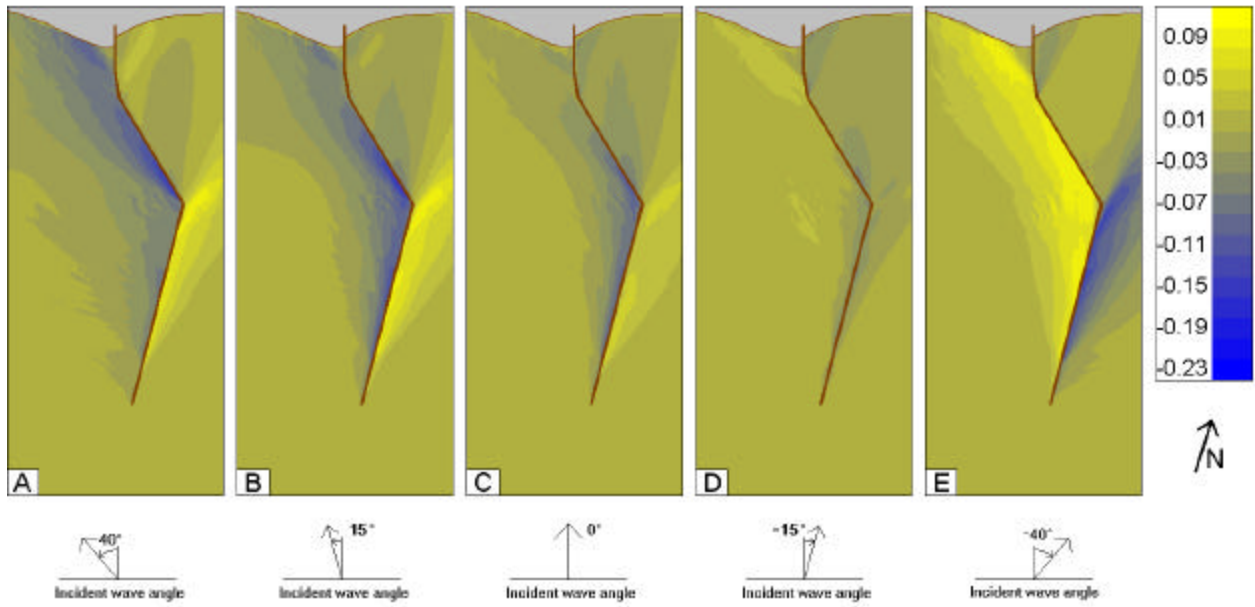


Figure A 6 - Height Differences for 50 ft vs. Existing Channel for 11.5 sec Period Waves, Cases 26-30.

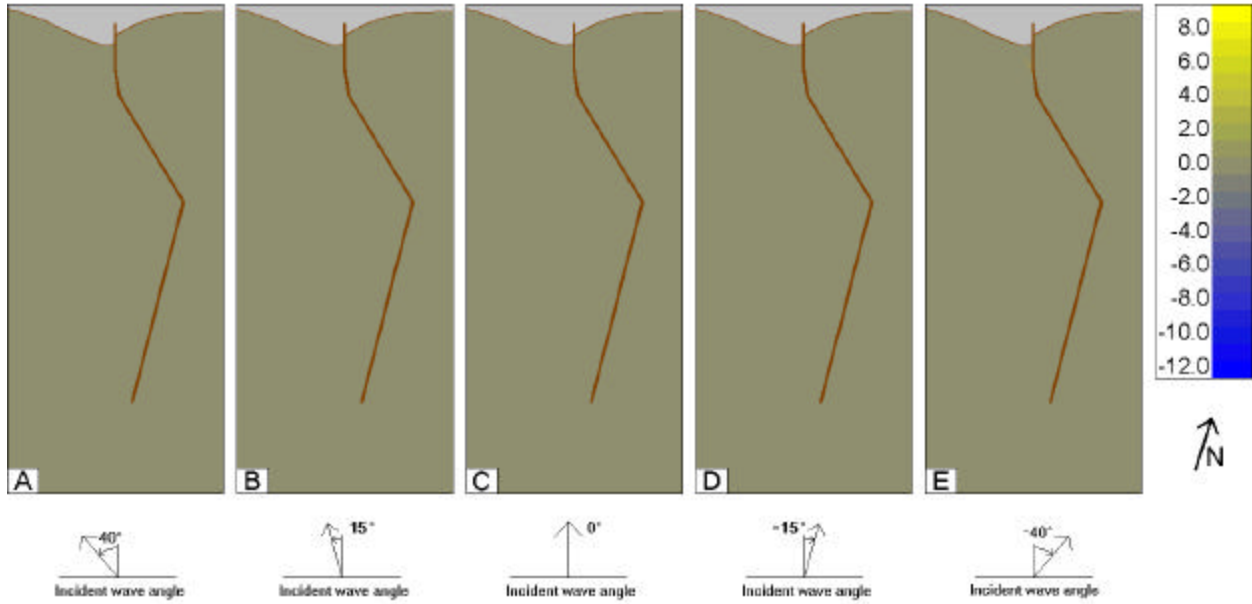


Figure A 7 - Wave Angle Changes for 50 ft vs. Existing Channel for 3.8 sec Period Waves, Cases 1-5. Bright yellow indicates areas where wave crests will be rotated in a counter-clockwise direction relative to their orientation with the existing channel, blue indicates areas of clockwise rotation, and muddy yellow-blue indicates areas of no relative rotation. The scale on the right hand side indicates the rotation in degrees.

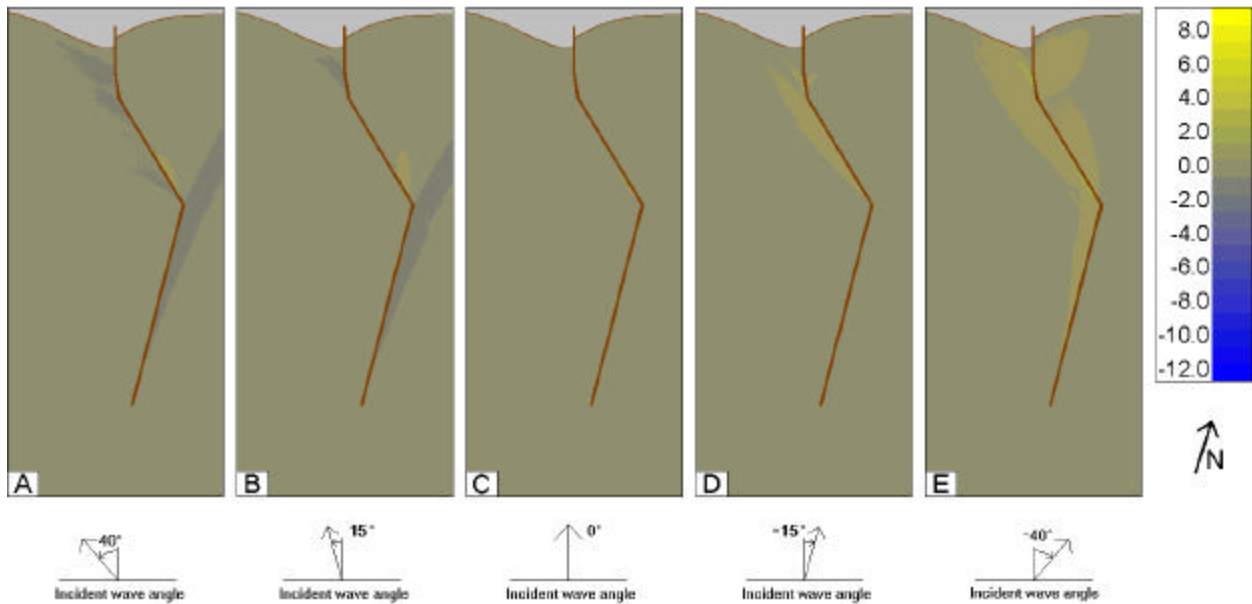


Figure A 8 - Wave Angle Changes for 50 ft vs. Existing Channel for 4.9 sec Period Waves, Cases 6-10.

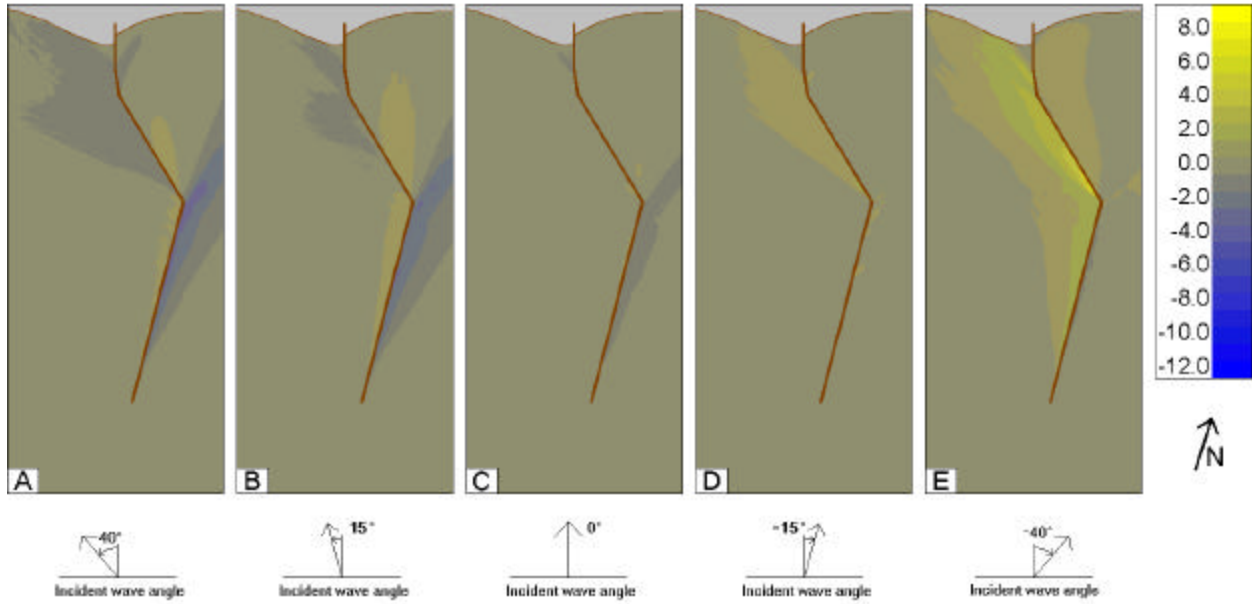


Figure A 9 - Wave Angle Changes for 50 ft vs. Existing Channel for 6.0 sec Period Waves, Cases 11-15.

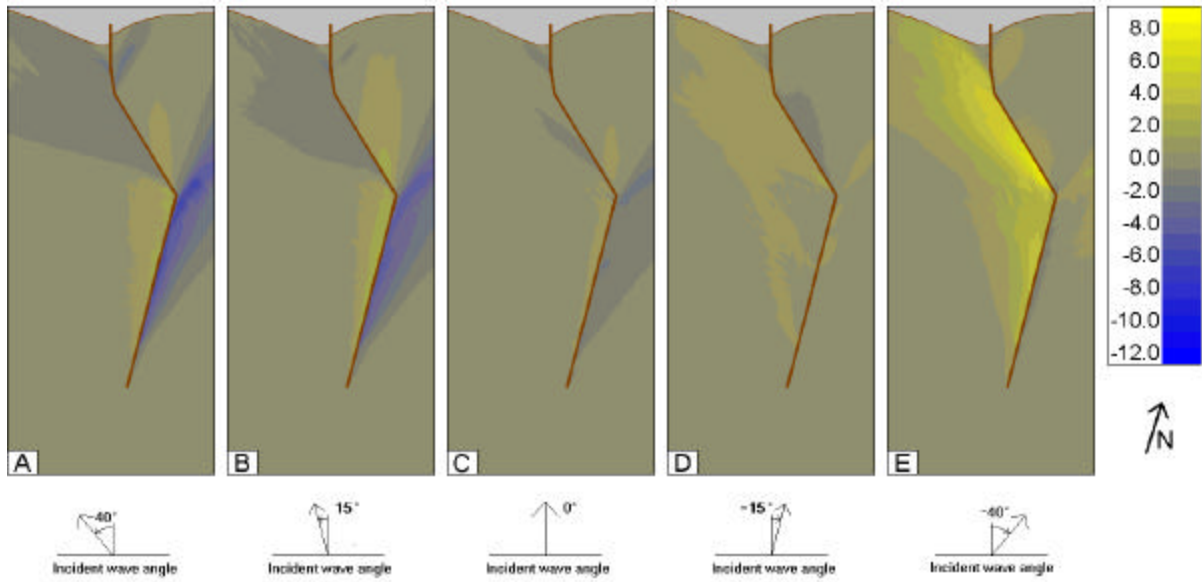


Figure A 10 - Wave Angle Changes for 50 ft vs. Existing Channel for 7.6 sec Period Waves, Cases 16-20.

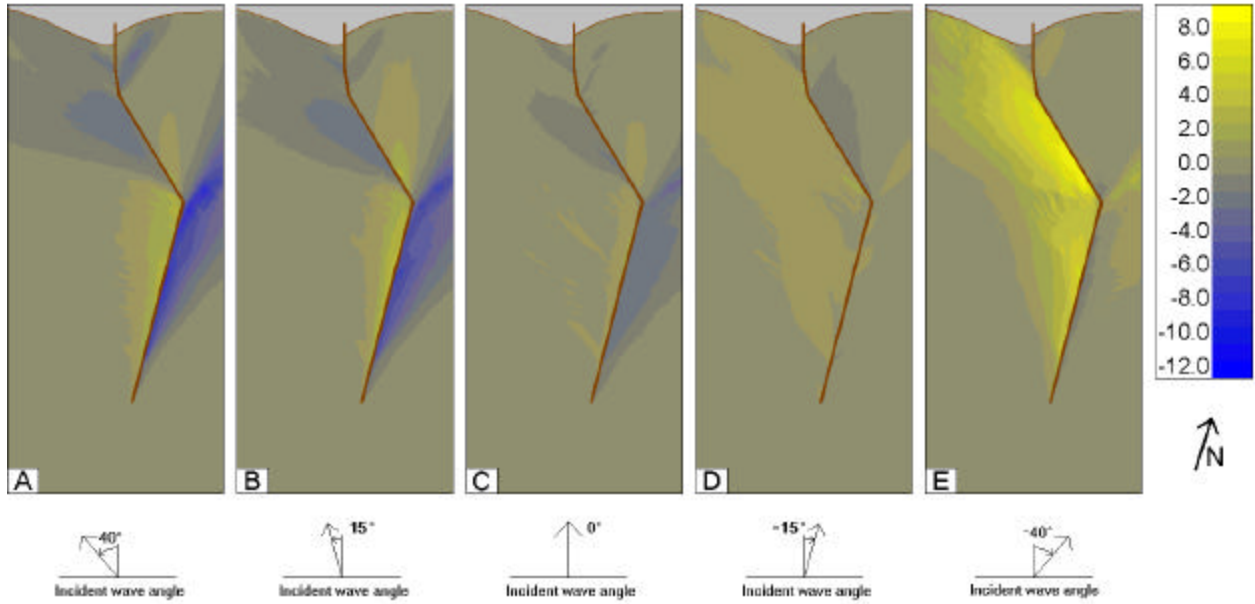


Figure A 11 - Wave Angle Changes for 50 ft vs. Existing Channel for 9.5 sec Period Waves, Cases 21-25.

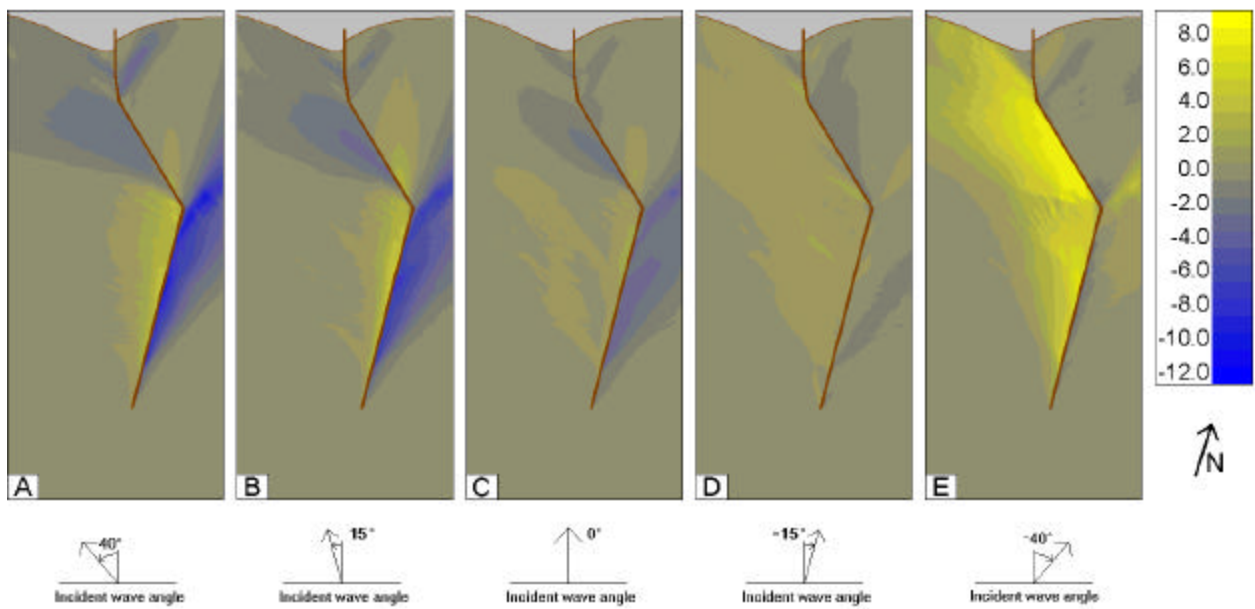


Figure A 12 - Wave Angle Changes for 50 ft vs. Existing Channel for 11.5 sec Period Waves, Cases 26-30.

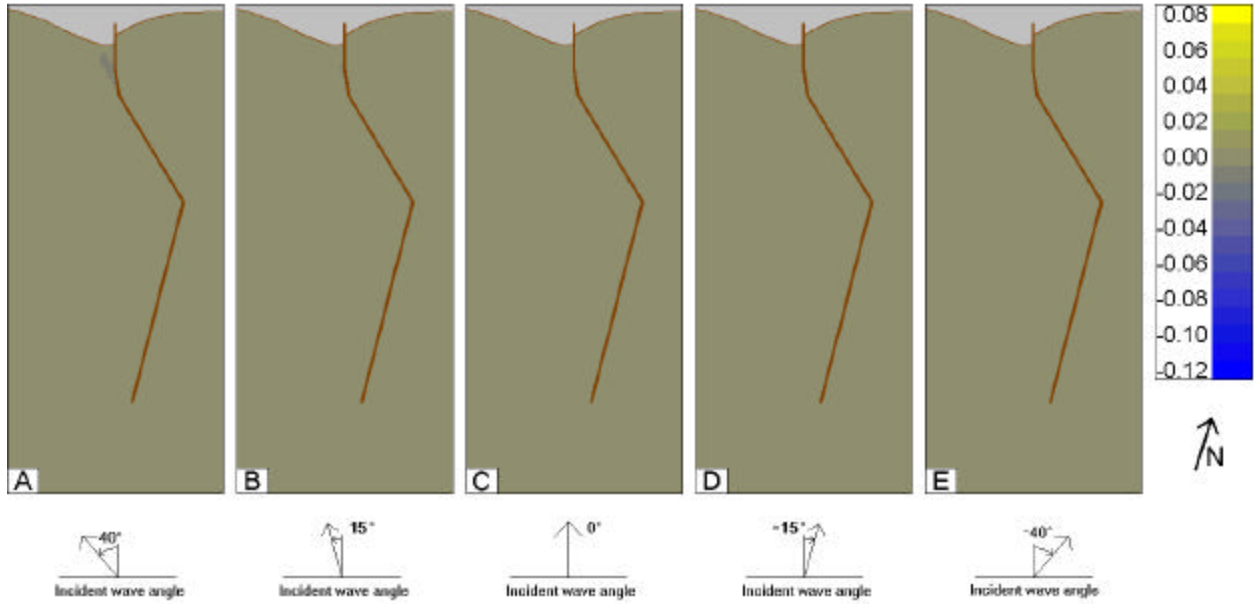


Figure A 13 - Height Differences for 45 ft vs. Existing Channel for 3.8 sec Period Waves, Cases 1-5. The scale on the right can be considered a percentage change from existing conditions. Note that the scale is different than in Figures A1-A6.

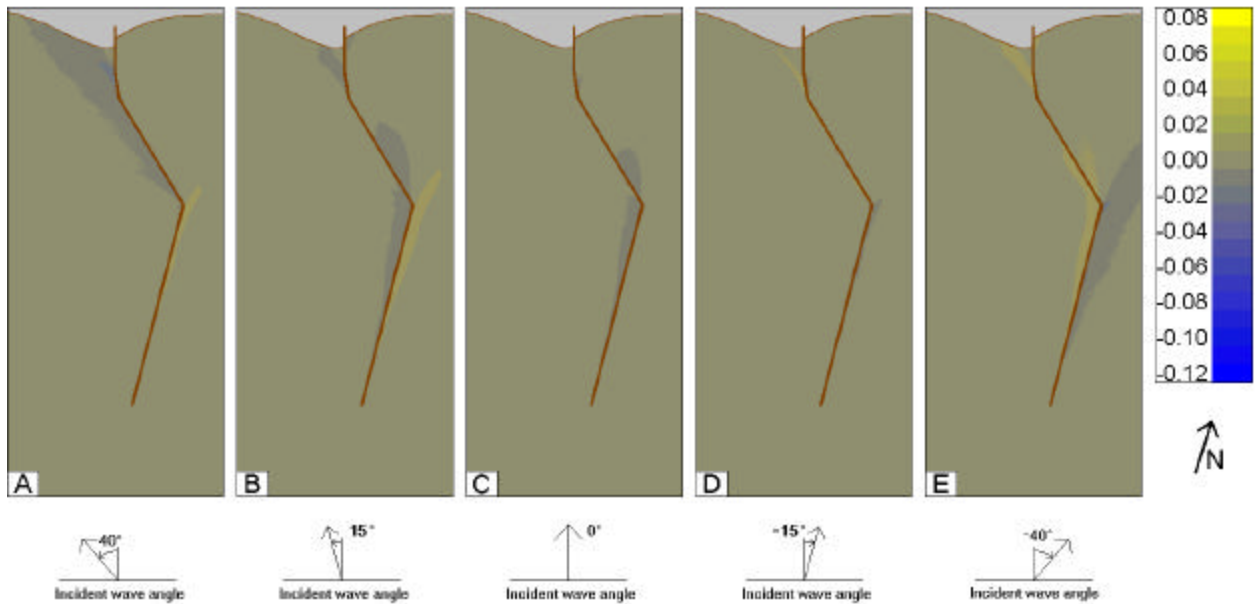


Figure A 14 - Height Differences for 45 ft vs. Existing Channel for 4.9 sec Period Waves, Cases 6-10.

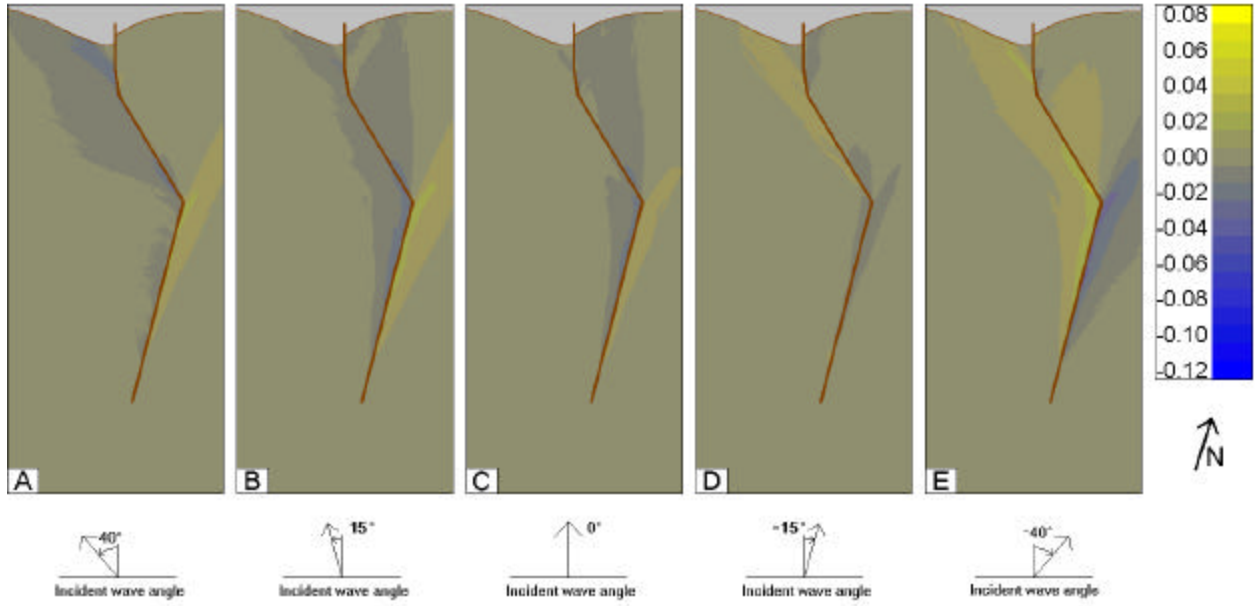


Figure A 15 - Height Differences for 45 ft vs. Existing Channel for 6.0 sec Period Waves, Cases 11-15.

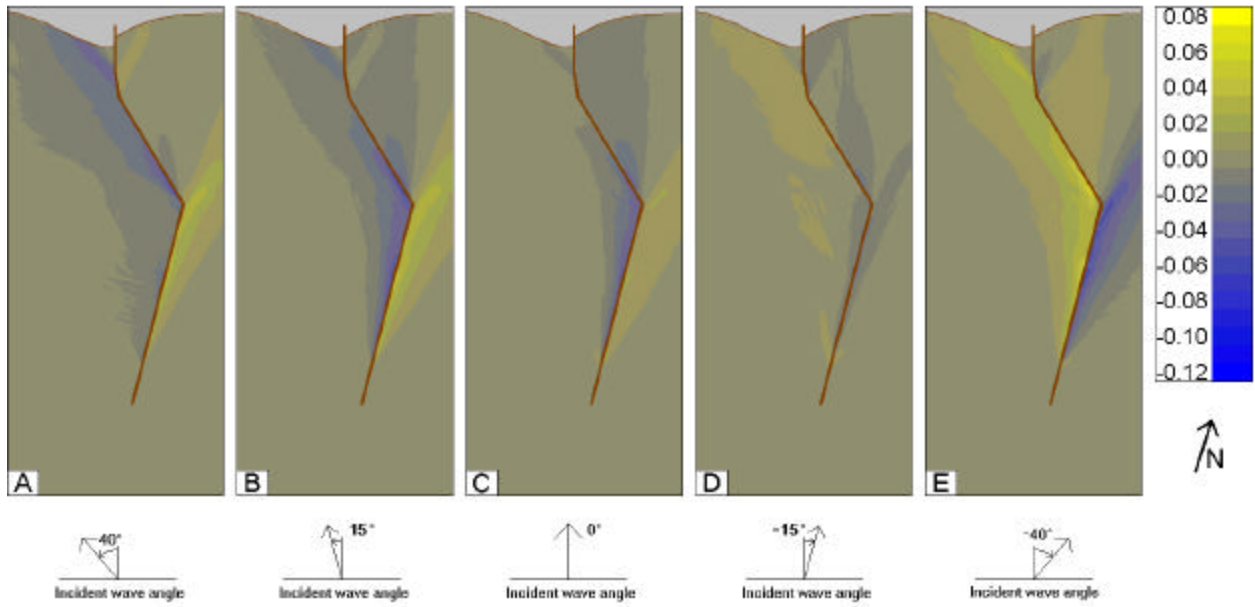


Figure A 16 - Height Differences for 45 ft vs. Existing Channel for 7.6 sec Period Waves, Cases 16-20.

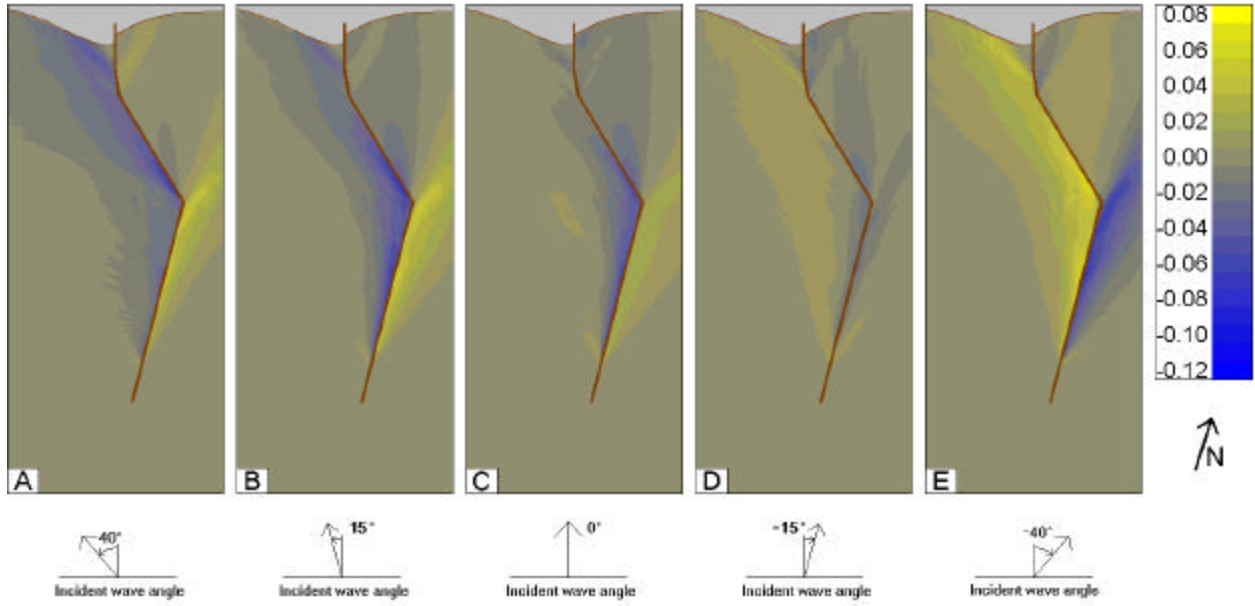


Figure A 17 - Height Differences for 45 ft vs. Existing Channel for 9.5 sec Period Waves, Cases 21-25.

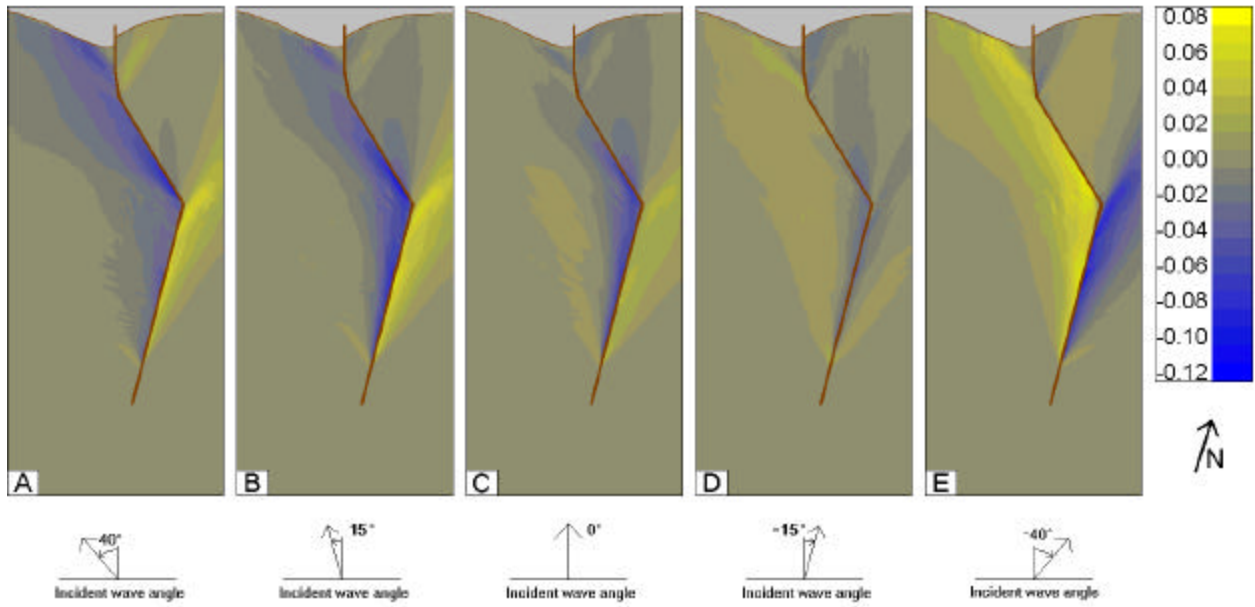


Figure A 18 - Height Differences for 45 ft vs. Existing Channel for 11.5 sec Period Waves, Cases 26-30.

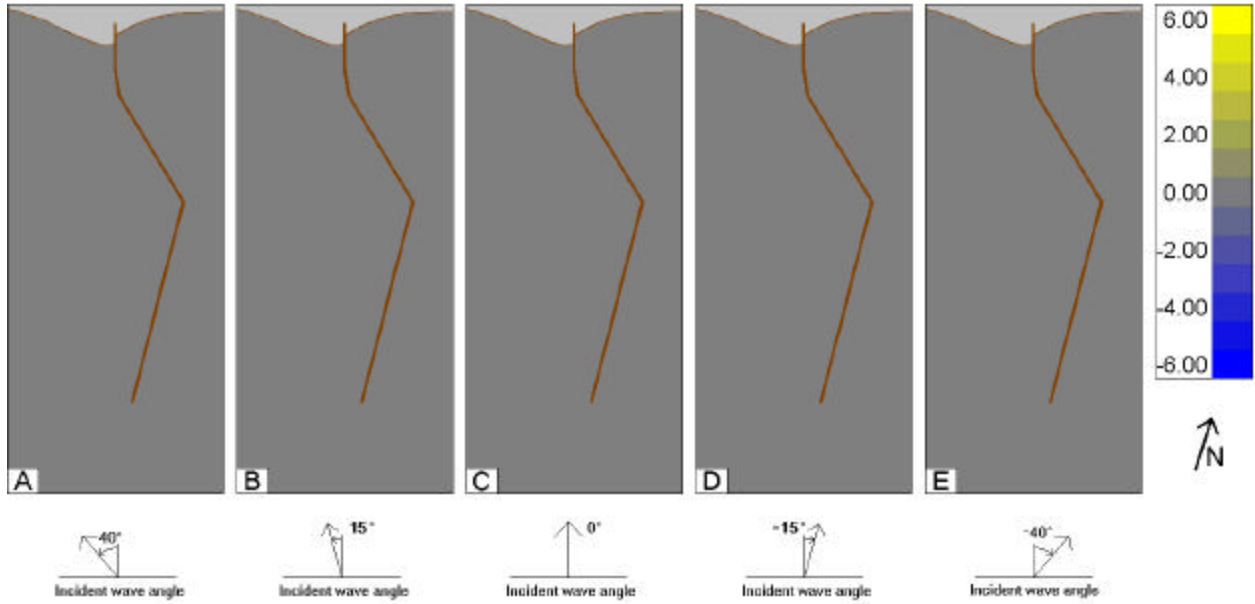


Figure A 19 - Wave Angle Changes for 45 ft vs. Existing Channel for 3.8 sec Period Waves, Cases 1-5. The scale on the right hand side indicates the rotation in degrees. Note that the scale is different than in Figures A7-A12.

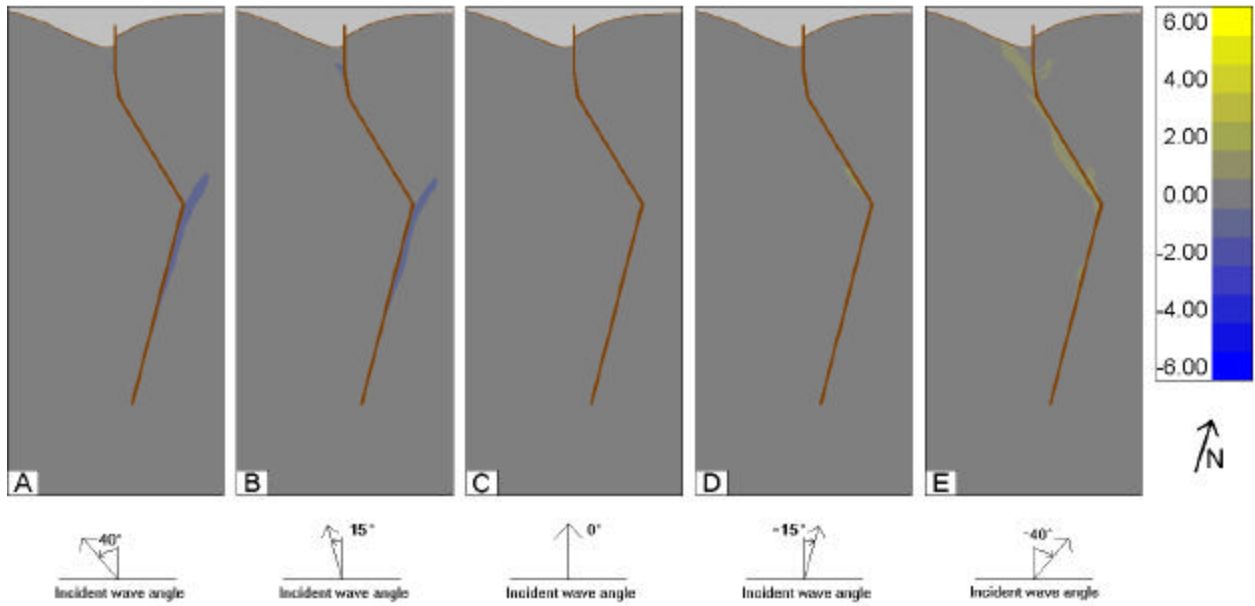


Figure A 20 - Wave Angle Changes for 45 ft vs. Existing Channel for 4.9 sec Period Waves, Cases 6-10.

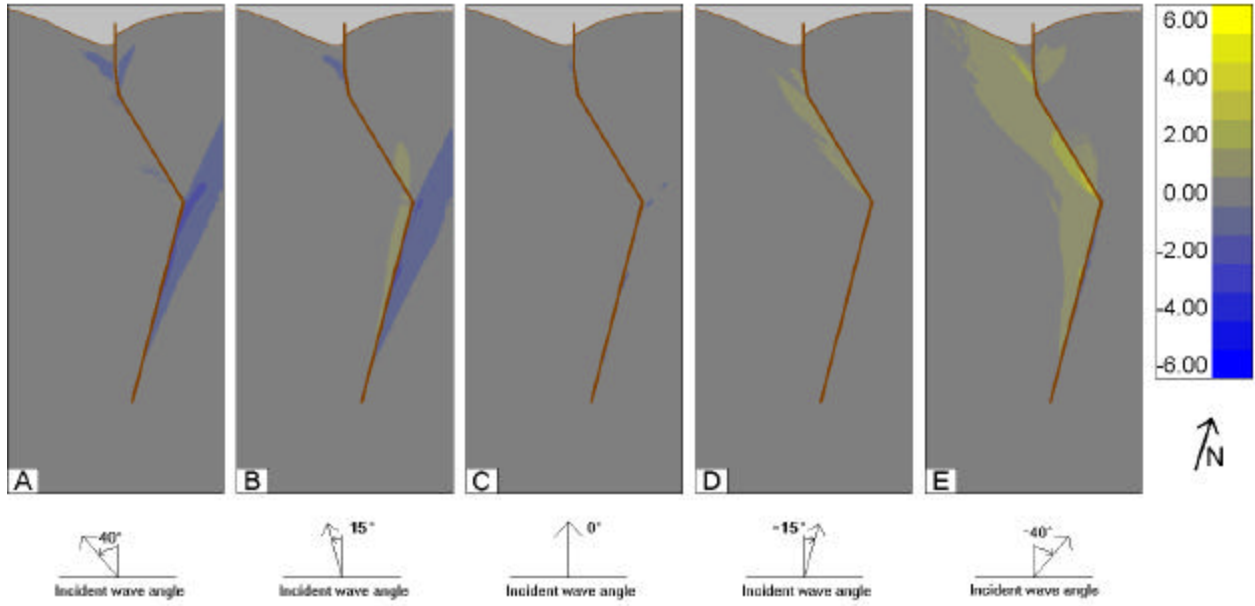


Figure A 21 - Wave Angle Changes for 45 ft vs. Existing Channel for 6.0 sec Period Waves, Cases 11-15.

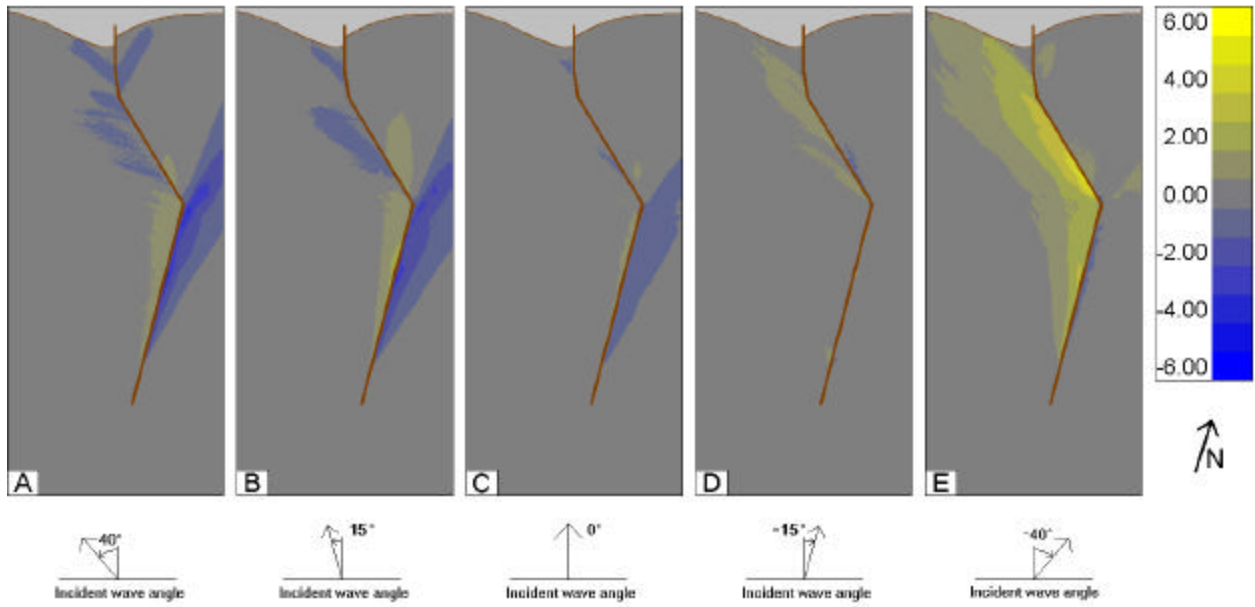


Figure A 22 - Wave Angle Changes for 45 ft vs. Existing Channel for 7.6 sec Period Waves, Cases 16-20.

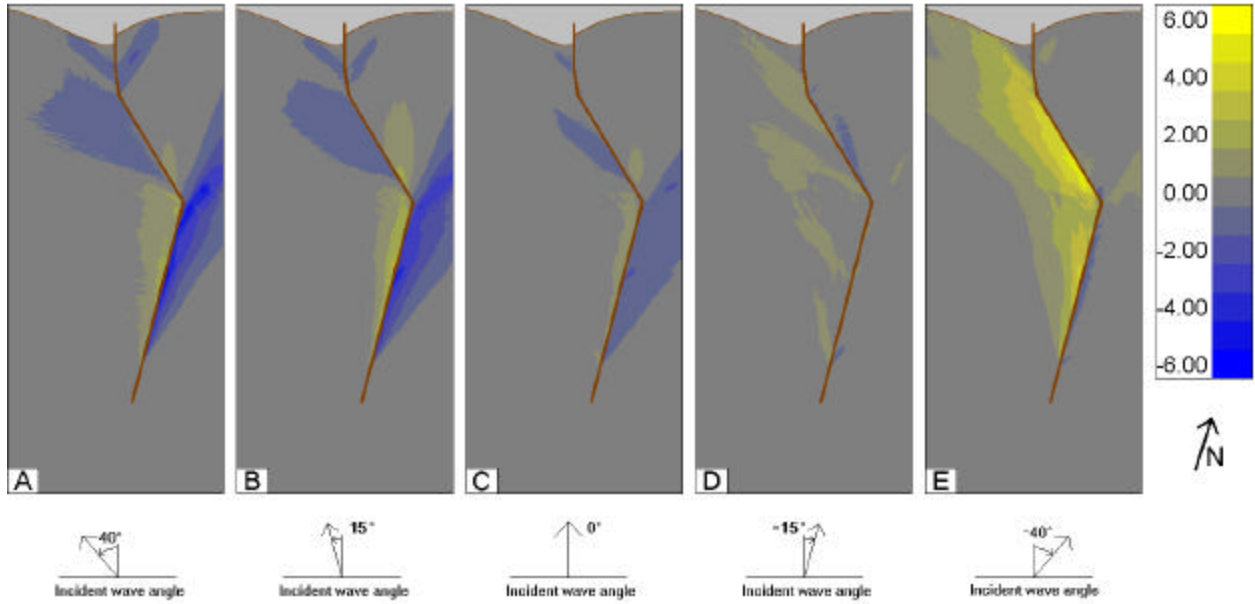


Figure A 23 - Wave Angle Changes for 45 ft vs. Existing Channel for 9.5 sec Period Waves, Cases 21-25.

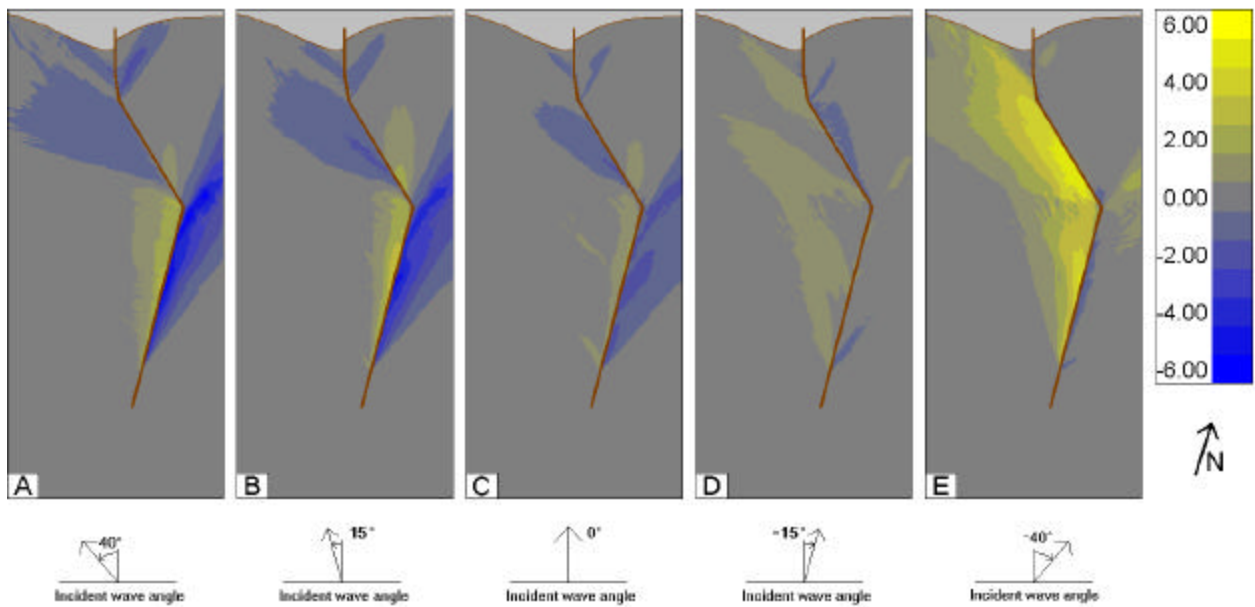


Figure A 24 - Wave Angle Changes for 45 ft vs. Existing Channel for 11.5 sec Period Waves, Cases 26-30.